

PARTICLE SIZE MEASUREMENT
USING LIQUID EXCLUSION CHROMATOGRAPHY

MEASUREMENT OF PARTICLE SIZE IN THE SUBMICRON
RANGE - EVALUATION OF LIQUID EXCLUSION CHROMATOGRAPHY (LEC)

Measurement of Particle Size in the Submicron
Range - Evaluation of Liquid Exclusion Chromatography (LEC)

by

Surendra Singh

A Thesis Submitted to the
Faculty of Graduate Studies in the Partial
Fulfilment of the Requirements for the
Degree Master of Engineering

©Surendra Singh 1977

McMaster University

October 1977

Master of Engineering (1977)
(Chemical Engineering)

McMaster University
Hamilton, Ontario

TITLE: Measurement of Particle Size in the Submicron Range
- Evaluation of Liquid Exclusion Chromatography (LEC)

AUTHOR: SURENDRA SINGH, M.Sc. (Org. Chem.), Ph.D. (Phy-org. Chem.)

SUPERVISOR: Professor A.E. Hamielec

NUMBER OF PAGES: VIII, 94

ABSTRACT:

Herein is reported a theoretical and experimental evaluation of liquid exclusion chromatography (LEC) for the measurement of particle size distribution (PSD) and diameter averages for colloidal spheres of various compositions.

Correction factors for axial dispersion have been derived for a general detector whose signal is proportional to the number of particles times particle diameter to the power gamma (γ) where γ varies from zero to six. This general detector includes a turbidimeter ($\gamma=6$) and a refractometer ($\gamma=3$).

Equipment and operational variables and their effect on resolution were investigated experimentally. These included packing and pore sizes, bed length and carrier liquid flowrate.

The use of LEC for the off-line monitoring of the growth of latex particles was investigated for the surfactant-free emulsion polymerization of two monomer systems-styrene and vinyl acetate.

LEC can be used to quantitatively measure the size distribution and diameter averages of both organic latices and inorganic particles in the submicron range in an off-line analytical mode. LEC is sufficiently rapid for the off-line monitoring of latex particle growth in emulsion

polymerization. With some modification it could be used in an online mode as a sensor for reactor control.

ACKNOWLEDGEMENTS

I wish to express my deep sense of gratitude
to Prof. A.E. Hamielec for his help and guidance, indispensable
for the successful completion of this thesis,
to the Department of Chemical Engineering of McMaster University
for financial assistance,
to L. Garcia for his help in writing the computer program,
to Debbie McCreathe for typing the entire thesis.

TABLE OF CONTENTS

| | <u>Page</u> |
|--|-------------|
| ABSTRACT | |
| 1. INTRODUCTION | 1 |
| 2. LITERATURE SURVEY | 3 |
| 2.1 Measurement of Particle Size Distribution (PSD) and Averages in the Submicron Range | 3 |
| 2.1.1 Introduction | 3 |
| 2.1.2 Electron Microscopy | 3 |
| 2.1.3 Joyce Loeb Disc Centrifuge | 4 |
| 2.1.4 Light Scattering | 5 |
| (A) Turbidity Spectra | 6 |
| (B) Dissymmetry Method | 6 |
| 2.1.5 Column Chromatography | 6 |
| (A) Hydrodynamic Chromatography (HDC) | 6 |
| (B) Liquid Exclusion Chromatography (LEC) | 6 |
| (C) Mechanisms (LEC vs. HDC) | 6 |
| 3. THEORETICAL DEVELOPMENT | 9 |
| 3.1 Interpretation of Signal from a UV Detector | 9 |
| 3.2 Axial Dispersion Corrections for a General Detector | 11 |
| 3.2.1 Numerical Solution | 12 |
| 3.2.2 Analytical Solution | 13 |
| (A) Rayleigh Scattering | 15 |
| (B) Mie Scattering | 20 |

| | <u>Page</u> |
|---|-------------|
| 4. EXPERIMENTAL DETAILS | 22 |
| 4.1 Apparatus | 22 |
| 4.2 Column Packing | 23 |
| 4.3 Operational Variables Investigated | 24 |
| 4.4 Application in Emulsion Polymerization | 25 |
| 4.4.1 Styrene Emulsion Polymerization | 26 |
| 4.4.2 Vinyl Acetate Emulsion Polymerization | 26 |
| 5. RESULTS AND DISCUSSIONS | 27 |
| 5.1 Resolution | 27 |
| 5.2 Correction for Axial Dispersion | 29 |
| 5.3 Particle Growth in Emulsion Polymerization | 30 |
| 6. CONCLUSION AND RECOMMENDATIONS | 33 |
| 7. NOMENCLATURE | 34 |
| 8. REFERENCES | 72 |
| 9. APPENDICES | 74 |
| 9.1 Technique for Following the Monomer Concentration in Aqueous and in Polymer Phase of an Emulsion or Suspension Polymerization | 74 |
| 9.2 Method to Evaluate Frequency Distribution Function, Variance and Total Number of Particles Using Turbidities at Two Different Wavelengths | 75 |
| 9.3 Computer Program | 77 |



LIST OF FIGURES

- FIGURE 1 Diagrammatic Representation of Mechanisms of Particle Separation by Liquid Exclusion Chromatography (LEC) and Hydrodynamic Chromatography (HDC)
- FIGURES 2-8 Particle Diameter - Retention Volume Calibration Curve
- FIGURES 9,10 Effect of Solvent Flow Rate on the Particle Diameter - Retention Volume Calibration Curve
- FIGURES 11,12 Effect of Solvent Flow Rate on Variance of Chromatograms for Single Diameter Species
- FIGURE 13(a) Conversion-time History for the Surfactant-Free Emulsion Polymerization of Styrene at 70.5 °C
- FIGURE 13(b) Particle Diameter-time History for the Surfactant-Free Emulsion Polymerization of Styrene at 70.5 °C
- FIGURE 14(a) Conversion-time History for the Surfactant-Free Emulsion Polymerization of Vinyl Acetate at 85°C
- FIGURE 14(b) Particle Diameter-time History for the Surfactant-Free Emulsion Polymerization of Vinyl Acetate at 85°
- FIGURE 15(a) Concentration of Vinyl Acetate in Aqueous and Polymer Phases versus Time for an Emulsion Polymerization of Vinyl Acetate with Continuous Monomer Addition
- FIGURE 15(b) Conversion-time History for the Emulsion Polymerization of Vinyl Acetate with Continuous Monomer Addition
- FIGURE 16 Scattering Coefficient vs. Particle Diameter

LIST OF TABLES

| | |
|--------------|---|
| TABLE 1 | Correction Factors for Different Diameter Averages for a Turbidity Detector in the Rayleigh Scattering Regime and for a Refractometer for Gaussian Axial Dispersion |
| TABLE 2 | Axial Dispersion Correction Factors for a General Detector Including a Skewing Correction Term |
| TABLE 3 | Column Packing Used for Evaluation of Liquid Exclusion Chromatography (LEC) |
| TABLE 4 | Particle Standards used for Evaluation of Liquid Exclusion Chromatography |
| TABLE 5 | Values of $(D_{20}^2)^2$ for Polystyrene Standard (1000 \AA°) with Different Column Combinations. |
| TABLES 6-10 | Effect of Solvent Flowrate on the Variance for Polystyrene Standards |
| TABLE 11 | Reproducibility of Peak Position and Chromatogram Variance for Polystyrene Standard (1000 \AA°) |
| TABLE 12 | Different Diameter Averages for Polystyrene Standard (1000 \AA°) Corrected for Axial Dispersion Using Analytical Solution with Mie Theory |
| TABLES 13-15 | Different Diameter Averages for Standards Corrected for Axial Dispersion Using Analytical Solution |
| TABLE 16 | Different Diameter Averages for Samples with Known Polydispersity |
| TABLE 17 | Measured Variances of LEC Chromatograms for the Surfactant-Free Emulsion Polymerization of Styrene at 70.5°C |
| TABLE 18 | Measured Variances of LEC Chromatograms for Surfactant-Free Emulsion Polymerization of Vinyl Acetate at 85°C |
| TABLE 19 | Normalized Heights of the Chromatograms for a Latex Sample at Two Different Wavelengths Using a Turbidity Detector |
| TABLE 20 | Corrected Diameter Averages for the Polystyrene Sample Whose Chromatograms were Obtained at Two Different Wavelengths Using a Turbidity Detector |

CHAPTER 1

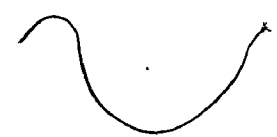
INTRODUCTION

The analysis of particle size or the particle size distribution is of vital concern to many different technologies ranging from the manufacture of paint to the formulation of the drugs and phytochemicals.

The importance of this physical characteristic is realized when one examines the chemical and physical properties controlled by particle size and distribution, eg. (i) the gloss of a film is a function of the particle size and distribution where normally the finer the particles and the more uniform the distribution, the higher the gloss, (ii) behaviour of some of the pharmaceutical tablets and capsules are now known to be controlled by the granular size of the substance used (1) (iii) not only the setting of the cement is controlled by the particle size but also are the mechanical properties of the cement.

The characteristics of a single particle are not usually of practical interest, rather the mean characteristics of a large number of particles is the thing that can be studied statistically. Particle sizing technique should, whenever possible duplicate the process one wishes to control eg. particle diameter of a catalyst is irrelevant especially if the material is very porous. Measurement of total area would be more appropriate. It is therefore essential to choose the right tool for the job at hand. Most methods of analysis measure different parameters, quite apart from intrinsic inaccuracies, so that the measurement of the properties of one system by different methods may give different results, all of which could be correct, eg. turbidity measurement yields diameter average based on

weight whereas electron microscope gives the number average diameter.



CHAPTER 2

LITERATURE SURVEY

There seems to be a widespread interest in methods for determining the particle size and size distribution. Methods of analysis vary from the direct microscope analysis to the indirect methods that depend on intrinsic or optical properties of the particles themselves. Different methods for particle size measurement have been discussed extensively in the recent literature (1, 2) and will not be discussed here except a few techniques that measure particle size distribution and averages in the submicron range.

2.1 Measurement of Particle Size Distribution (PSD) and Averages in the Submicron Range

2.1.1 Introduction

A few analytical techniques that are commonly used for particle size analysis in the submicron range are discussed briefly along with their merits and demerits. Techniques for measuring particle size distribution in this range tend to be either time consuming, inaccurate or limited to a portion of the total size range.

2.1.2 Electron Microscope

A drop of highly dilute suspension (10^{-3} - 10^{-5} gm/ml) is placed on a collodin coated screen of about 200 mesh and allowed to dry. The dried specimen is then examined in the microscope and particles photographed and from the magnification employed number average particle size

can be computed (2). Diameter averages other than number average can also be obtained by integrating the histogram. This technique can be applied to samples with narrow or broad particle size distribution.

Some of the modern electron microscopes have magnification as high as 500000x and the resolution of the order of 2-7 Å°.

One of the main problems in electron microscopy is to get representative sample eg. a dispersion at a concentration of 50 wt. % made up of 2000 Å° particles can have over 10^{13} particles/ml. Depending upon the polydispersity of the sample normally 500-2000 particles are counted. Since it is a very tedious and time consuming task to count couple of thousand particles and measure their size and hence the magnitude of the problem is obvious.

The temperature of the sample in the electron microscope is about 100°C but can reach as high as 200-275°C. Under these conditions the particles may shrink.

Above all this method is time consuming and expensive and requires highly trained technicians to obtain the data.

2.1.3 Joyce Loebl Disc Centrifuge

The principle of Joyce Loebl Disc Centrifuge system combines that of sedimentation with centrifugation (2). The suspension is centrifuged for certain time and then the suspension is sampled at a given distance into the fluid where Stoke's law predicts the presence of particles smaller than a given diameter and measuring concentration. From this data a distribution graph of particle diameter against percentage cumulative weight under size can be obtained. Some of the modern centrifuges are equipped

with a photosedimentometer attachment which eliminates the need for concentration analysis. Photosedimentometer measures the rate of sedimentation in the sample chamber by monitoring the attenuation of a light beam as the particles are sedimenting.

The advantage here is that any sample that can be centrifuged can be analyzed but one must know the density of the particles very accurately. The disc centrifuge is difficult to use with particles smaller than 1000 Å because the analysis time becomes too long considering the stability of the instrument.

2.1.4 Light Scattering

A dilute suspension is illuminated by a narrow intense beam of monochromatic light. The intensity of light is measured by means of a suitable detector at some angle θ from the primary beam.

For non-absorbing, non-interacting spherical particles the light scattering is a function of two parameters $\alpha (= \frac{\pi D}{\lambda m})$ and $m (= \frac{n}{n_0})$ (3). The particle size of the sol and its refractive index will govern the observed intensities. The three most common approaches to the measurement of particle size are

- A. fix θ at 180° and measure I . This is the turbidity measurement,
- B. Measure I at some other fixed angle. This is known as dissymmetry method,
- C. Measure I as a function of angle.

Turbidity measurement and dissymmetry methods are discussed briefly in the following sections.

A. Turbidity Spectra

The technique involves measurement of turbidity as a function of wavelength for a dilute suspension of non-absorbing spherical particles (4). In principle it is possible to obtain both the particle number and size distribution through measurement of turbidity as a function of wavelength but in fact it is difficult to find a unique distribution function without prior knowledge of the shape of the particle size distribution. In the Rayleigh Scattering regime a measurement of τ versus λ will provide only a turbidity average diameter and not the particle size distribution itself.

The advantage of this method lies in its experimental simplicity.

B. Dissymmetry Method

In the dissymmetry technique the intensity of scattered light at two different angles symmetrical around $\theta = 90^\circ$ is measured (4). Generally θ is taken as 45° and 135° . The scattering of light by particles is described by a series of differential equations for electromagnetic radiation. Solution of these equation by the Mie Theory gives a quantitative relationship between the diameter of the particle and the ratio of the intensities of scattered light.

This technique is useful for particles with diameter up to about 2000 Å.

2.1.5 Size Exclusion Chromatography

In the past decade, gel permeation chromatography (GPC) has been used extensively for the separation of polymer molecules according to

their size in solution. Recently, this technique has been adapted for analogous separation of colloidal dispersions according to size (5,6,7).

There are two complementary approaches to the use of size exclusion chromatography to separate particle suspensions according to size. The more powerful technique called liquid exclusion chromatography (LEC) utilizes porous packing and relies mainly on steric exclusion from the pores of the packing for size separation. The other called hydrodynamic chromatography (HDC) mainly developed by Hamish Small (5) utilizes non-porous packing and relies mainly on the velocity profile in the interstitial regions for size separation.

Krebs and Wunderlich (8) were the first to succeed in separating polymethylmethacrylate and polystyrene latex particles using silica gel having very large pores ($500-50000 \text{ \AA}^{\circ}$). More recently, Gaylor et al. (7) and Coll et al. (10) developed LEC further by suitable selection of emulsifier and electrolyte concentrations to optimize resolution.

The basic separating mechanisms in LEC and in HDC are discussed in the following section.

Mechanism (LEC vs. HDC)

The development of HDC is based on the theory proposed by Guttman and DiMarzio (9). More recently it has been developed further by Stoisits et al. (10) and McHugh (11). On the other hand there does not seem to be any literature dealing with the quantitative development of LEC.

The basic separating mechanisms of LEC and HDC are compared diagrammatically in Figure 1. A bed packed with porous or non-porous packing presents the particles suspended in the carrier solvent with a tortuous

path through a large number of capillary-like tunnels. Larger particles are excluded from regions near the capillary wall where axial velocities are small and hence on the average experience a higher velocity and therefore a smaller retention time.

Porous packing presents an additional force for size separation by steric exclusion from the pores. Figure 1(A) represents a wide interstitial channel and slot like pore. Suspended particles smaller than the diameter of the pore, can diffuse into pores giving a second and more efficient mechanism of retardation and size separation.

It has been suggested that the flow pattern of the solvent in the interstitial channels also plays an important role in chromatographic separation (12).

Cassassa (13) has pointed out that it is not possible to make phenomenological distinction between the separating mechanisms of LEC and HDC and it is likely that both mechanisms are operable with or without porous packing.

CHAPTER 3

THEORETICAL DEVELOPMENTS

3.1 Interpretation of a Signal for a UV Detector

In the absence of multiple scattering and for a non-absorbing monodisperse spherical suspension the turbidity (τ), is related to particle number (N) (4) by the following equation

$$\tau = N \frac{\pi D^2}{4} \times K\left(\frac{D}{\lambda_m}, \frac{n}{n_m}\right) \quad (1)$$

The turbidity is found by measuring the intensity of transmitted light using the following expression

$$\tau = \frac{1}{\ell} \ln \frac{I_0}{I} \quad \text{where } I_0 \text{ is the intensity of the primary beam}$$

I is the intensity of the transmitted beam

ℓ is the path length of the cell

Therefore for a polydisperse suspension of spheres, linear combination of equation (1) gives an integral equation of the form

$$\tau = N \int_0^\infty K\left(\frac{D}{\lambda_m}, \frac{n}{n_m}\right) \times \frac{\pi D^2}{4} \times f(D) dD$$

In the Mie scattering regime where $1.0 < \alpha < 10.0$, the dependence of extinction coefficient on α is complex. In the Rayleigh scattering regime where α is less than unity, the extinction coefficient is given by

the following analytical expression

$$K = \frac{8}{3} \left(\frac{m^2 - 1}{m^2 + 2} \right)^2 \alpha^4 \quad \text{where } m = \frac{n}{n_m} \\ \alpha = \frac{\pi D}{\lambda} \frac{m}{m}$$

Substituting this expression in equation (1) one obtains

$$\tau = B N D^6$$

where

$$B = \frac{2}{3} \frac{\pi}{4} \frac{5}{\lambda} \left(\frac{m^2 - 1}{m^2 + 2} \right)^2$$

Hence with Rayleigh scattering the turbidity τ at any point on the LEC chromatogram can be expressed as follows

$$\tau(v) = B N(v) D^6(v)$$

since

$F(v) \propto \tau(v)$ where $F(v)$ is the detector response

$$F(v) = B N(v) D^6(v)$$

$$N(v) = \frac{1}{B} \frac{F(v)}{D^6(v)} \quad (2)$$

Therefore, the total number of particles under the whole chromatogram can be obtained by integrating equation (2)

$$N = \frac{1}{B} \int_0^\infty F(v) D^{-6}(v) dv$$

Since the frequency distribution

$$f(D) dD = - \frac{N(v)}{N} dv$$

$$f(D) = \frac{F(v) D^{-6}(v)}{\int_0^\infty F(v) D^{-6}(v) dv} \frac{dv}{dD} \quad (3)$$

Similarly, one can derive an expression using the Mie theory

$$f(D) = \frac{F(v) K^{-1}(v) D^{-2}(v)}{\int_0^\infty F(v) K^{-1}(v) D^{-2}(v) dv} \frac{dv}{dD} \quad (4)$$

Given the frequency distribution, one can calculate the weight fraction distribution as follows

$$w(D) = \frac{D^3 f(D)}{\int_0^\infty D^3 f(D) dD} \quad (5)$$

3.2 Axial Dispersion Corrections for a General Detector

As with other forms of chromatography, the LEC chromatogram of a monodisperse suspension appears as a chromatogram of finite width. The peak position of the chromatogram is characteristic of the diameter of the suspension. In case of a refractometer, the area under the chromatogram is proportional to the mass of the monodisperse suspension injected and the variance of the chromatogram depends on band spreading mainly in the LEC columns. For a polydisperse suspension, the chromatogram is a superposition of the chromatograms of all its components. The total area under the curve is still proportional to the mass of the suspension injected, but now the height of the chromatogram at any retention volume does not depend solely upon the mass of one component, but also depends on the masses of the

the neighbouring components. At the tails of the chromatograms, there are chromatogram heights representing components which do not exist in the sample. For accurate particle size analysis this overlapping and diffused pattern of the chromatogram which results due to axial dispersion must be corrected.

Axial dispersion corrections in size exclusion chromatography of suspensions are much larger than for polymer molecules in solution. This is due to the fact that suspended particles in the submicron range are much larger than polymer molecules in solution and as a consequence have much smaller diffusion coefficients. Axial dispersion is greater with LEC than with HLC and is a result of the finite time required for a particle to diffuse into and out of a pore.

Tung (14) was the first to develop a method to correct for axial dispersion in GPC. Accounting for axial dispersion the detector response $F(v)$ of an input sample $W(y)$ is given by the following integral equation which is known as the Tung's Integral Equation

$$F(v) = \int_0^{+\infty} W(y) G(v,y) dy \quad (6)$$

where $G(v,y)$ is the instrumental spreading function and accounts for axial dispersion. Tung's equation can be solved numerically or analytically and both of these techniques are discussed briefly in the following section (15).

3.2.1 Numerical Solution

For a Gaussian instrumental spreading function $G(v,y)$ can be expressed as

$$G(v,y) = \frac{1}{\sqrt{2\pi}\sigma^2} \exp\left(-\frac{(v-v_0)^2}{2\sigma^2}\right)$$

where v is the retention volume, v_0 is the peak retention volume and σ^2 is the variance of a single species chromatogram. For a polydispersed suspension $F(v)$ can be represented as

$$F(v) = \int_0^\infty W(y) \frac{1}{\sqrt{2\pi}\sigma^2} \exp\left(-\frac{(v-y)^2}{2\sigma^2}\right) dy \quad (7)$$

In equation (7) the function $W(y)$ can be solved for numerically given $F(v)$ (via detector) and σ^2 (via calibration). There are many numerical techniques available in the literature for the solution of equation (7) and these are discussed elsewhere (15, 16). It is also possible to solve equation (7) numerically using non-Gaussian instrumental spreading functions.

3.2.2 Analytical Solution

Numerical solution of Tung's equation is not completely satisfactory in cases where corrections for axial dispersion are appreciable. Artificial maxima in the corrected $W(y)$ are often observed. Such maxima would lead to incorrect interpretation and hence can not be tolerated.

Tung's equation for the special case of a uniform instrumental spreading function becomes a convolution integral of the form

$$I(v) = \int_0^\infty W(y) G(v-y) dy \quad (8)$$

Here the instrumental spreading function is considered to be uniform i.e.

the normalized detector signals for single diameter species may be superimposed. Taking the Laplace Transform of equation (8) gives

$$\bar{F}(s) = \bar{W}(s) \bar{G}(s) \quad (9)$$

Provder and Rosen (17) proposed the use of a general statistical shape function to describe instrumental spreading. This function which accounts for derivation from Gaussian shape, has the following form.

$$G(v) = \phi(v) + \sum_{n=3}^{\infty} (-1)^n \frac{A_n \phi^n(v)}{[n(\sqrt{\frac{1}{\sigma^2}})]^n}$$

where $\phi(v) = \frac{1}{\sqrt{2\pi\sigma^2}} \text{Exp}(-\frac{v^2}{2\sigma^2})$ and $\phi^n(v)$ denotes the nth order derivatives. The coefficients A_n are functions of the nth order moments about the mean retention volume. The coefficient A_3 provides a measure of skewness and it is this term which will be used to correct for derivations from the instrumental spreading function from the Gaussian shape. Equation (9) can now be written as

$$\bar{F}(s) = \bar{W}(s) \text{Exp}(-\frac{s^2\sigma^2}{2}) \left(1 + \sum_{n=3}^{\infty} \frac{A_n}{[n]} (-s\sigma)^n\right)$$

and neglecting the terms other than A_3

$$\bar{F}(s) = \bar{W}(s) \text{Exp}(-\frac{s^2\sigma^2}{2})(1 - \alpha s^3) \quad (10)$$

$$\text{where } \alpha = \frac{1}{6} A_3 \sigma^3$$

Equation (10) is the basis for axial dispersion corrections of spherical particles of various particle diameter averages to follow.

Axial dispersion correction factors will be derived for a general detector whose signal $F(v)$ is proportional to the number of particles in the detector cell times the diameter of the particles to the power γ

$$\text{i.e. } F(v) \propto N(v) D(v)^\gamma$$

when $\gamma = 6$, the detector is measuring turbidity in the Rayleigh scattering regime and when $\gamma = 3$, the signal is proportional to the mass of the suspension and independent of the particle diameter. The frequency distribution ($f(D)$) can be expressed as follows

$$\begin{aligned} f(D) dD &= \frac{N(v) dv}{\int_0^\infty N(v) dv} \\ &= \frac{F(v) D(v)^{-\gamma} dv}{\int_0^\infty F(v) D(v)^{-\gamma} dv} \end{aligned}$$

A. Rayleigh Scattering

Axial dispersion correction factors for different diameter averages are derived for a general detector. When $\gamma = 6$, the correction factors apply for the Rayleigh Scattering regime.

Correction factor for number average diameter -

Now the number average diameter can be expressed as follows

$$D_n(\infty) = \frac{\int_0^\infty D(v) F(v) D(v)^{-\gamma} dv}{\int_0^\infty F(v) D(v)^{-\gamma} dv}$$

In terms of Laplace Transformations after introducing the linear calibration curve of the form $D(v) = D_1 \text{Exp}(-D_2 v)$, $D_n(\infty)$ and $D_n(t)$ can be expressed as follows

$$D_n(\infty) = D_1 \frac{\bar{F}((1-\gamma)D_2)}{\bar{F}(-\gamma D_2)}$$

$$D_n(t) = D_1 \frac{\bar{W}((1-\gamma)D_2)}{\bar{W}(-\gamma D_2)}$$

and therefore the correction factor is

$$\frac{D_n(t)}{D_n(\infty)} = \frac{\bar{W}((1-\gamma)D_2)}{\bar{F}((1-\gamma)D_2)} \times \frac{\bar{F}(-\gamma D_2)}{\bar{W}(-\gamma D_2)}$$

Introducing equation (10) one obtains

$$\frac{D_n(t)}{D_n(\infty)} = \text{Exp} \left\{ \frac{(2\gamma-1)D_2^2 \sigma^2}{2} \right\} \left\{ \frac{1+\gamma^3 \alpha D_2^3}{1-(1-\gamma)^3 \alpha D_2^3} \right\}$$

Correction factor for surface area average diameter

One can derive the correction factors for different diameter averages, as shown earlier

$$D_s(\infty) = \left\{ \frac{\int_{\infty}^{\infty} D^2(v) F(v) D(v)^{-\gamma} dv}{\int_{\infty}^{\infty} F(v) D(v)^{-\gamma} dv} \right\}^{1/2}$$

$$D_s(\infty) = D_1 \left\{ \frac{\bar{F}((2-\gamma)D_2)}{\bar{F}(-\gamma D_2)} \right\}^{1/2}$$

$$D_s(t) = D_1 \left\{ \frac{\bar{W}((2-\gamma)D_2)}{\bar{W}(-\gamma D_2)} \right\}^{1/2}$$

Hence

$$\frac{D_s(t)}{D_s(\infty)} = \left\{ \frac{\bar{W}((2-\gamma)D_2)}{\bar{F}((2-\gamma)D_2)} \times \frac{\bar{F}(-\gamma D_2)}{\bar{W}(-\gamma D_2)} \right\}^{1/2}$$

$$\frac{D_s(t)}{D_s(\infty)} = \text{Exp}\{(y-1)D_2^2\sigma^2\} \left\{ \frac{1+\gamma^3 \alpha' D_2^3}{1-(2-\gamma)^3 \alpha' D_2^3} \right\}^{1/2}$$

Correction factor for specific surface area average diameter -

$$D_{ss}(\infty) = \frac{\int_0^\infty D^3(v) F(v) D(v)^{-\gamma} dv}{\int_0^\infty D^2(v) F(v) D(v)^{-\gamma} dv}$$

$$D_{ss}(\infty) = D_1 \frac{\bar{F}((3-\gamma)D_2)}{\bar{F}((2-\gamma)D_2)}$$

$$D_{ss}(t) = D_1 \frac{\bar{W}((3-\gamma)D_2)}{\bar{W}((2-\gamma)D_2)}$$

$$\frac{D_{ss}(t)}{D_{ss}(\infty)} = \frac{\bar{W}((3-\gamma)D_2)}{\bar{F}((3-\gamma)D_2)} \times \frac{\bar{F}((2-\gamma)D_2)}{\bar{W}((2-\gamma)D_2)}$$

$$\frac{D_{ss}(t)}{D_{ss}(\infty)} = \text{Exp}\left((2y-5)\frac{D_2^2\sigma^2}{2}\right) \left(\frac{1-(2-\gamma)^3 \alpha' D_2^3}{1-(3-\gamma)^3 \alpha' D_2^3} \right)$$

Correction factor for weight average diameter -

$$D_w(\infty) = \frac{\int_0^\infty D^4(v) F(v) D(v)^{-\gamma} dv}{\int_0^\infty D^3(v) F(v) D(v)^{-\gamma} dv}$$

$$D_w(\infty) = D_1 \frac{\bar{F}((4-\gamma)D_2)}{\bar{F}((3-\gamma)D_2)}$$

$$D_w(t) = D_1 \frac{\bar{W}((4-\gamma)D_2)}{\bar{W}((3-\gamma)D_2)}$$

$$\frac{D_w(t)}{D_w(\infty)} = \frac{\bar{W}((4-\gamma)D_2)}{\bar{F}((4-\gamma)D_2)} \times \frac{\bar{F}((3-\gamma)D_2)}{\bar{W}((3-\gamma)D_2)}$$

$$\frac{D_w(t)}{D_w(\infty)} = \exp \left(\frac{(2\gamma-7)D_2^2 \sigma^2}{2} \right) \left\{ \frac{1-(3-\gamma)^3 \alpha D_2^3}{1-(4-\gamma)^3 \alpha D_2^3} \right\}$$

Correction factor for volume average diameter -

$$D_v(\infty) = \left\{ \frac{\int_0^\infty D^3(v) F(v) D(v)^{-\gamma} dv}{\int_0^\infty F(v) D(v)^{-\gamma} dv} \right\}^{1/3}$$

$$D_v(\infty) = D_1 \left(\frac{\bar{F}((3-\gamma)D_2)}{\bar{F}(-\gamma D_2)} \right)^{1/3}$$

$$D_V(t) = D_1 \left(\frac{\bar{W}((3-\gamma)D_2)}{\bar{W}(-\gamma D_2)} \right)^{1/3}$$

$$\frac{D_V(t)}{D_V(\infty)} = \left\{ \frac{\bar{W}((3-\gamma)D_2)}{\bar{F}((3-\gamma)D_2)} \times \frac{\bar{F}(-\gamma D_2)}{\bar{W}(-\gamma D_2)} \right\}^{1/3}$$

$$\frac{D_V(t)}{D_V(\infty)} = \text{Exp}\left(\frac{(2\gamma-3)D_2^2\sigma^2}{2}\right) \left\{ \frac{1+\gamma^3 \alpha' D_2^3}{1-(3-\gamma)^3 \alpha' D_2^3} \right\}^{1/3}$$

Correction factor for turbidity average diameter

$$D_\tau(\infty) = \left\{ \frac{\int_0^\infty D^6(v) F(v) D(v)^{-\gamma} dv}{\int_0^\infty D^3(v) F(v) D(v)^{-\gamma} dv} \right\}^{1/3}$$

$$D_\tau(\infty) = D_1 \left\{ \frac{\bar{F}((6-\gamma)D_2)}{\bar{F}((3-\gamma)D_2)} \right\}^{1/3}$$

$$D_\tau(t) = D_1 \left\{ \frac{\bar{W}((6-\gamma)D_2)}{\bar{W}((3-\gamma)D_2)} \right\}^{1/3}$$

$$\frac{D_\tau(t)}{D_\tau(\infty)} = \left\{ \frac{\bar{W}((6-\gamma)D_2)}{\bar{F}((6-\gamma)D_2)} \times \frac{\bar{F}((3-\gamma)D_2)}{\bar{W}((3-\gamma)D_2)} \right\}^{1/3}$$

$$\frac{D_\tau(t)}{D_1(\infty)} = \text{Exp}\left(\frac{(2\gamma-9)D_2^2\sigma^2}{2}\right) \left\{ \frac{1-(3-\gamma)^3 \alpha' D_2^3}{1-(6-\gamma)^3 \alpha' D_2^3} \right\}^{1/3}$$

The correction factors for the different averages are tabulated in Tables 1 and 2.

B. Mie Scattering

Derivation of the correction factors for the turbidity detector for the more general Mie Scattering regime now follows. Here the signal $F(v)$ is proportional to

$$F(v) \propto N(v) K(v) D^2(v)$$

The frequency distribution can now be given by

$$\begin{aligned} f(D) dD &= \frac{N(v) dv}{\int_0^\infty N(v) dv} \\ &= \frac{F(v) K^{-1}(v) D^{-2}(v) dv}{\int_0^\infty F(v) K^{-1}(v) D^{-2}(v) dv} \end{aligned}$$

Referring to number average as an example

$$D_n(t) = \frac{\int_0^\infty W(v) K^{-1}(v) D^{-1}(v) dv}{\int_0^\infty W(v) K^{-1}(v) D^{-2}(v) dv}$$

To maintain Laplace Transformation to permit the use of equation (10), one must fit extinction coefficients with a series which is the sum of exponentials. Therefore,

$$D_n(t) = D_1 \frac{\sum_i \bar{W}(s_i)}{\sum_j \bar{W}(s_j)}$$

$$D_n(t) = D_1 \frac{\sum_i \bar{F}(s_i)/\bar{G}(s_i)}{\sum_j \bar{F}(s_j)/\bar{G}(s_j)}$$

CHAPTER 4

EXPERIMENTAL DETAILS

4.1 Apparatus

The instrumentation for LEC is the same as that for GPC. Mainly it consists of (i) Sample injection valve, (ii) Pump, (iii) Columns, (iv) Detector, (v) Effluent volume detection and data recording (usually a strip chart recorder).

Sample Injection Valve:

The conventional six port two way injection valve, manufactured by Disc Instruments Inc. was used. This valve was designed to withstand hydrostatic pressures of up to 5000 psi. The volume of the sample loop was 2 ml.

Pump:

Positive displacement pump (Milton Roy Mini Pump Model 396-89) with an adjustable delivery volume was used for pumping the solution which could deliver up to 7.6 ml/min even at back pressures of up to 5000 psi. Pressure fluctuations were damped out with an inline pulse damper.

Columns:

A set of columns (4' x 3/8") each packed with porous silica and/or porous glass were used. Details of the packing materials are given in Table 3.

Detector:

Initially a pharmacia UV-spectrophotometer with a cell of 10 mm path length was used at 254 nm wavelength. Later, a Waters Associates Model 440 Absorbance detector was used for monitoring simultaneously turbidities at two wavelengths.

Effluent Volume Detector:

To monitor the volume of the effluent through the column as a function of time, a siphon (along with a Waters Associates Liquid Volume Indicator), that discharges when full and at each discharge sends a signal, to the recorder where a blip is recorded, was used. In fact this arrangement is simple, but it is prone to error, eg. evaporation from siphon and effluent continuing to flow into the siphon while it is discharging. More recently Bly (18) has reported a technique whereby error due to flowrate variations can be eliminated.

Data Recording:

The signal from the detector and the effluent volume counter was recorded on a standard strip chart recorder.

4.2 Column Packing

Dry packing material was poured into the top of the column while the column was being vibrated with an electric vibrator. A vacuum line was attached to the lower end of the column to ensure better packing. The column was vibrated until no change in the bed volume was seen.

Carrier solvent was pumped through the column and a vacuum line

was attached to the other end of the column. The solvent was allowed to flow and the vacuum was applied off and on for about half an hour. After this the carrier fluid was allowed to flow continuously through it for about 24 hours before the column was ready to be used.

4.5 Operational Variables Investigated

A. Carrier Solvent

The carrier liquid was water which contained 1 gm/l Aerosol O.T. (BDH Lab Reagent Grade) and 1 gm/l of potassium nitrate (Baker Chemical Co.). This carrier liquid was recommended by Coll et al. (6). No further attempts at optimizing surfactant and electrolyte type or levels was attempted in this investigation.

B. Particle Standards

Monodispersed particles with known diameter and with different chemical composition were used as standards for determining the particle diameter - retention volume calibration curve. Standards specifications are tabulated in Table 4.

C. Pore Size and the Particle Diameter of the Packing Material

Columns were packed with packing materials having wide range of pore sizes ($30,000 \text{ A}^\circ$ to 100 A°) and particle sizes (125μ to 5μ). Packing materials with large particle size (75μ - 125μ) and with large pore size ($10,000$ - $30,000 \text{ A}^\circ$) increase the axial dispersion without improving the peak separation appreciably. Similarly, packing materials with pore sizes smaller than 800 A° do not increase the peak separation either. Packing

materials with $5-10\mu$ particle size resulted in column plugging and therefore they are not recommended for particle suspensions. Optimum resolution (for particle size analysis of samples with particles smaller than 3000 \AA°) was achieved by using packing materials with $37-74\mu$ particle size and with $2500-1500 \text{ \AA}^\circ$ pore size.

D. Carrier Solvent Flowrate

The effect of carrier solvent flowrate on the particle diameter-retention volume calibration curve was investigated between $0.9 \frac{\text{ml}}{\text{min}}$ to $7.5 \frac{\text{ml}}{\text{min}}$. The upper bound of the flowrate study was limited by the capacity of the pump employed in this study.

E. Analysis Technique

The detector gave a steady baseline within about 20 mins after the chromatograph was switched on.

Standards or the unknowns were diluted with the carrier fluid at room temperature, filtered through 0.8μ or 1.2μ filter paper and were then injected into the chromatograph. The typical solute charges were less than 5 mg. During any set of analyses the flowrate was maintained constant. The analysis time was of the order of 8-20 mins at 7.5 ml/min flowrate depending upon the set of columns being used.

4.4 Application of LEC in Emulsion Polymerization

To demonstrate the usefulness of LEC in following the growth of polymer particles in emulsion polymerization the following polymerizations were done.

4.4.1 Styrene Emulsion Polymerization

The surfactant-free emulsion polymerization of styrene was carried out at 70.5 °C in a 5-liter round bottom flask equipped with a condenser, stirrer, thermometer and nitrogen purge. Freshly distilled styrene (181 g) and distilled water (1990 g) were allowed to equilibrate in the reaction flask for 30 min under stirring and nitrogen purge. Potassium persulfate (1.995 g) was dissolved in 10 mL distilled water at 70°C and then added to the reaction flask. This immediately initiated the polymerization. Samples of the latex were withdrawn at specific times and the polymerization was stopped by cooling the sample with ice cold water. The diluted latex was then injected into the LEC. These polymerization conditions were almost identical to those used by Goodall et al. (19).

4.4.2 Vinyl Acetate Emulsion Polymerization

Surfactant-free emulsion polymerization of vinyl acetate was carried out at 85°C using the equipment and procedure described above. Freshly distilled vinyl acetate (25 mL), dimethyl ethanol amine (0.1 mL) and distilled water (695 mL) were charged into the reaction flask and allowed to equilibrate for 30 min at 85°C under stirring and nitrogen purge. Ammonium persulfate (1.042 g) was dissolved in 5 mL distilled water at 85°C and added to the reaction flask to initiate polymerization. Samples of the latex were withdrawn at different times, quenched and then injected into the LEC to follow polymer particle growth.

CHAPTER 5

RESULTS AND DISCUSSION

5.1 Resolution

The separating efficiency of a column or a set of columns can be determined by measuring the distance between the centers of the peaks of the two species and the base widths of the two peaks. The conventional definition of resolution (R) in chromatography is

$$R = \frac{2(V_2 - V_1)}{W_1 + W_2}$$

where V_1 , V_2 are the retention volumes of the species 1 and 2 respectively and W_1 , W_2 are the base widths of the two peaks. This definition of resolution is not very appropriate in the case of LEC because resolution decreases with increasing particle size. A more realistic approach would be to calculate some sort of resolution index that takes into consideration particle size and base width (15). The decrease in resolution for larger particles is due to the fact that fewer pores are available to the larger particles than are available to the smaller particles.

Separation in LEC is a function of the size range of the particles in the sample, the size range of the pores and the particle size of the packing material and how well a column is packed. Figures 2 to 8 show particle diameter-retention volume calibration curves with columns having different packing materials, but under similar solvent flow conditions. Figures 2, 3 and 4 show the calibration curve with the same set of columns but at different ages of the packing in the column.

It is obvious from these figures that the separation depends only on the size of the particle and not on the chemical composition. Pore geometry is an important factor to be optimized for improved separation, eg. deep interconnected pores will increase the axial dispersion unnecessarily. The extent to which the resolution can be increased, i.e. the extent to which the calibration curve can be flattened has certain limitations, eg. increasing the number of columns will increase the peak broadening. Hence it would be much more appropriate to look at the product of the slope of the calibration curve (D_2) and the variance of the single species chromatogram (σ^2) in order to describe the resolution of the column under investigation. Since the term $D_2 \sigma^2$ appears in the axial dispersion correction factors, hence $D_2 \sigma^2$ values were calculated for a polystyrene standard (1000 Å) with different sets of columns and the values are tabulated in Table 5. The lower the magnitude of $(D_2 \sigma^2)$, the higher the resolution. The effect of carrier fluid flowrate on peak separation and variance of single species chromatogram are plotted in Figures 9-12. It is of interest to note that the particle diameter-retention calibration curve was hardly affected by variations of flowrate from 0.94 ml/min to 7.5 ml/min. It seems as if the calibration curve shifts towards lower retention volumes by increasing the flowrate (see Figure 9). This is not true, however. This deviation is due to a change in siphon dump volume which changes because the solvent keeps flowing even when the siphon is discharging. Figure 10 shows the effect of change of solvent flowrate on the particle diameter-retention volume calibration curve after correcting for this error due to the change in siphon dump volume. It is obvious that the retention volume is essentially independent of flowrate from 0.9 to 7.5 ml/min. Figures

11 and 12 show the effect of change of flowrate on the variance of different monodispersed standards. Hence the resolution can be improved by lowering the flowrate. From a comparison of the slopes of the calibration curves of Figures 7 and 8 it is evident that packing material of size 37-74 μ gave much greater peak separation than those with 75-125 μ size packing material.

It can be concluded that for analysis for particles smaller than 3000 \AA° , one should have packing materials with pore size about 3000 \AA° and 1500 \AA° and a packing particle size 37-74 μ for optimum resolution.

5.2 Correction for Axial Dispersion

Table 1 shows the axial dispersion correction factors for different diameter averages for a turbidity detector in the Rayleigh Scattering regime and for a refractometer both with a Gaussian instrumental spreading function. It is of interest to note that the correction factors are always smaller for the refractometer than for the turbidity detector. This suggests that the refractometer would be a better detector than the turbidity detector. Even for the best resolution (i.e. when $D_{2\sigma}^2$ is minimum (Table 5)) the correction factors for D_n and D_s are of the order of 3.5-4 which is undesirably large. On the other hand the correction for D_t is relatively smaller (1.4). This suggests that the turbidity detector is probably not suitable for the determination of D_n and D_s via size exclusion chromatography.

Reproducibility of peak position and variance of one standard was checked under similar operating conditions and the results are tabulated in Table 11. The percent standard deviation for the diameter (from peak position) is quite small. Different diameter averages were calculated for these chromatograms and the values are listed in Table 12. The percent

standard deviation for the different averages calculated from these chromatograms is quite large, but this seems to be an inherent problem with this system. Tables 13-15 show the uncorrected and corrected diameter averages for samples of different sizes based on Rayleigh Scattering and on Mie Scattering. The calculated and the actual diameters agree better for smaller sized particles. LEC chromatograms of particles smaller than 1500 \AA° were found to be much more symmetrical than those larger than 1500 \AA° . Hence skewing correction had to be applied for larger particles. Table 13 shows the uncorrected and the corrected diameter averages for polystyrene standard (3120 \AA°) for Gaussian spreading and for skewed chromatogram. Table 16 shows the calculated diameter averages for some polydisperse samples.

As mentioned earlier in section 3.2.2(B), in order to apply the analytical correction for axial dispersion, scattering coefficient data should be expressed as the sum of exponentials of the form $\frac{i}{K(v)} = \text{Const 1 Exp (AV)} + \text{Const 2 Exp (BV)}$. Figure 16 depicts the actual values of the scattering coefficients along with those calculated from the exponential fit. Table 14 shows the uncorrected diameter averages calculated for a polystyrene standard (1000 \AA°) using the actual scattering coefficients and using the exponential fit. The agreement among these values is quite good.

5.5 Particle Growth in Emulsion Polymerization

In order to demonstrate the usefulness of this technique, a surfactant-free emulsion polymerization of styrene was carried out under similar conditions as those used by Goodall et al. (19). The size of the

polymer particles in emulsion polymerization at any time was obtained from the particle diameter-retention volume calibration curve shown in Figure 2, which was obtained by injecting monodisperse latices with known diameters under similar operating conditions of the chromatograph. The growth of the polystyrene particles measured by LEC was compared with the growth followed by electron microscopy and they are shown in Figure 13(b). The corresponding conversion-time history measured gravimetrically is shown in Figure 13(a). Excellent agreement is obtained between LEC and electron microscopy measurements. A typical auto-acceleration in polymerization rate at higher conversion due to diffusion-controlled termination is observed. As expected the growth rate of the particle diameter also accelerates for the same reason.

To show that LEC could be used to analyze soft latex particles (eg. Polyvinylacetate latices) as well as hard latex particles (eg. Polystyrene), growth rate of polymer particles of emulsion polymerization vinyl acetate was also followed. The conversion-time and particle diameter-time histories for the emulsion polymerization of vinyl acetate are shown in Figure 14. The results were once again as expected. The point to note here is that no difficulty was experienced in analyzing the polyvinylacetate latices that are rather soft compared to polystyrene latices.

One can obtain qualitative information about the polydispersity of the unknown sample by comparing the variance of the unknown sample with that of a sample with known polydispersity. Variances for LEC chromatograms for polystyrene and polyvinylacetate were calculated and they are tabulated in Tables 17 and 18 respectively. Table 17 shows that the variance decreases with increasing time and particle size. This is to be expected due to the nature of the emulsion polymerization where a finite time for nucleation is

required. The variances of the monodispersed standards are of the same order as those of the samples from the emulsion polymerization of polystyrene indicating that the polymer particles produced in this study are essentially monodispersed or at least as much so as the commercially available monodisperse standards. Goodall et al. (19) showed by electron microscopy that indeed the polystyrene particles were monodispersed. On the other hand the magnitude of the variances for polyvinylacetate polymer particles is larger indicating that the sample is not as monodispersed as the polystyrene latexes.

CHAPTER 6

CONCLUSIONS AND RECOMMENDATIONS

This study has shown that Liquid Exclusion Chromatography (LEC) is a very powerful technique for particle size analysis in the submicron range especially for particles smaller than 3000 Å. The analysis can be performed with satisfactory accuracy and in a matter of few minutes.

Future study should concentrate on using different kinds of detectors. For example, a detector whose signal is proportional to just the number of particles or to smaller powers of diameter unlike the turbidity detector should be developed. It will be of interest to compare the calculated diameter averages from a refractometer response with those of turbidity detection response.

CHAPTER 7

NOMENCLATURE

| | |
|---|--|
| N | Number of particles/liter |
| N(v) | Number of particles/liter at the retention volume v |
| D | Diameter of the particle |
| D(v) | Diameter of the particle eluting at volume v |
| $K(\frac{D}{\lambda_m}, \frac{n}{n_m})$ | Extinction coefficient and is a function of two dimensionless groups $\frac{D}{\lambda_m}$ and $\frac{n}{n_m}$ |
| λ_m | Wavelength of the light in the suspending medium |
| n | Refractive index of the particle |
| n_m | Refractive index of the suspending medium |
| τ | Turbidity |
| $\tau(v)$ | Turbidity at the retention volume v |
| I_o | Intensity of the primary beam |
| I | Intensity of the transmitted beam |
| ℓ | Path length of the cell |
| $f(D)$ | Frequency distribution |
| $F(D)dD$ | Number of particles in the diameter range $D-D+dD$ |
| $W(D)$ | Weight fraction distribution |
| α | $\pi D/\lambda_m$ |
| m | n/n_m |
| F(v) | Height of the LEC chromatogram at the retention volume v |
| B | Proportionality constant |

The different diameter averages were defined as follows:

$$D_n = \frac{\int_0^\infty D f(D) dD}{\int_0^\infty f(D) dD}$$

$$D_s = \left\{ \frac{\int_0^\infty D^2 f(D) dD}{\int_0^\infty f(D) dD} \right\}^{1/2}$$

$$D_{ss} = \frac{\int_0^\infty D^3 f(D) dD}{\int_0^\infty D^2 f(D) dD}$$

$$D_w = \frac{\int_0^\infty D^4 f(D) dD}{\int_0^\infty D^3 f(D) dD}$$

$$D_v = \left\{ \frac{\int_0^\infty D^3 f(D) dD}{\int_0^\infty f(D) dD} \right\}^{1/3}$$

$$D_t = \left\{ \frac{\int_0^\infty D^6 f(D) dD}{\int_0^\infty D^3 f(D) dD} \right\}^{1/3}$$

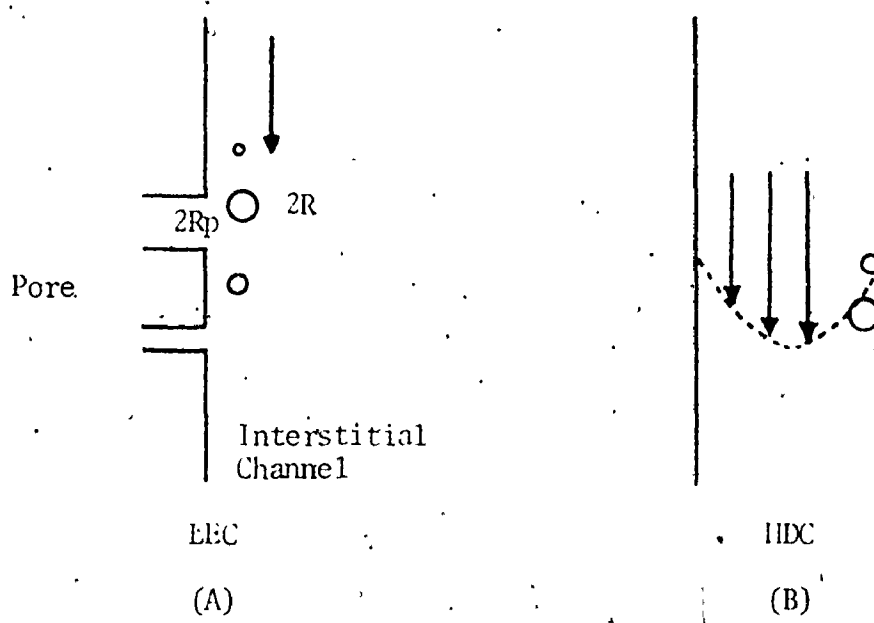


Figure 1: Diagrammatic representation of the mechanisms of separation by liquid exclusion chromatography (LEC) and hydrodynamic chromatography (HDC).

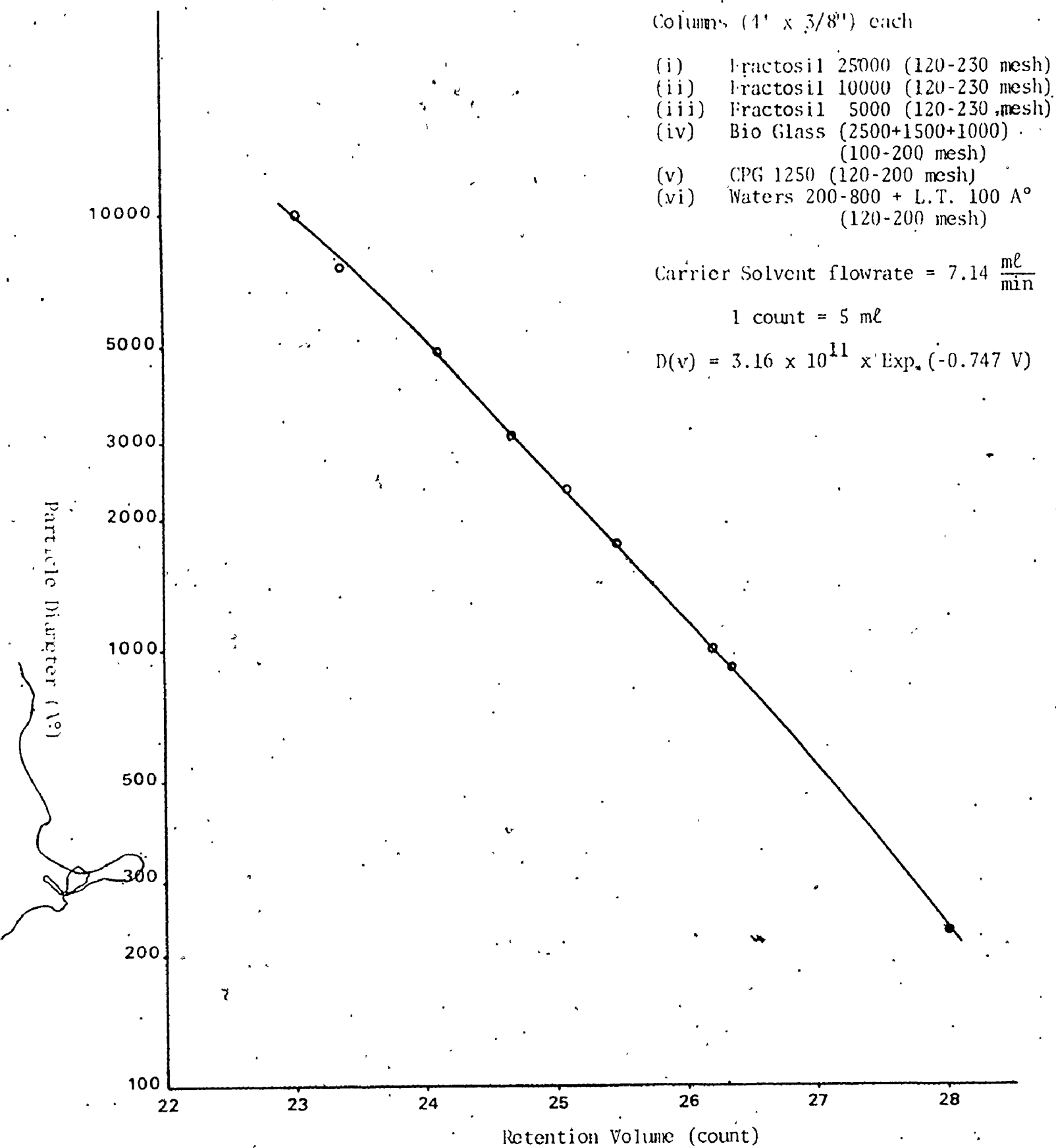


Figure 2: Particle diameter-retention volume calibration curve
○-PS, ●-silica

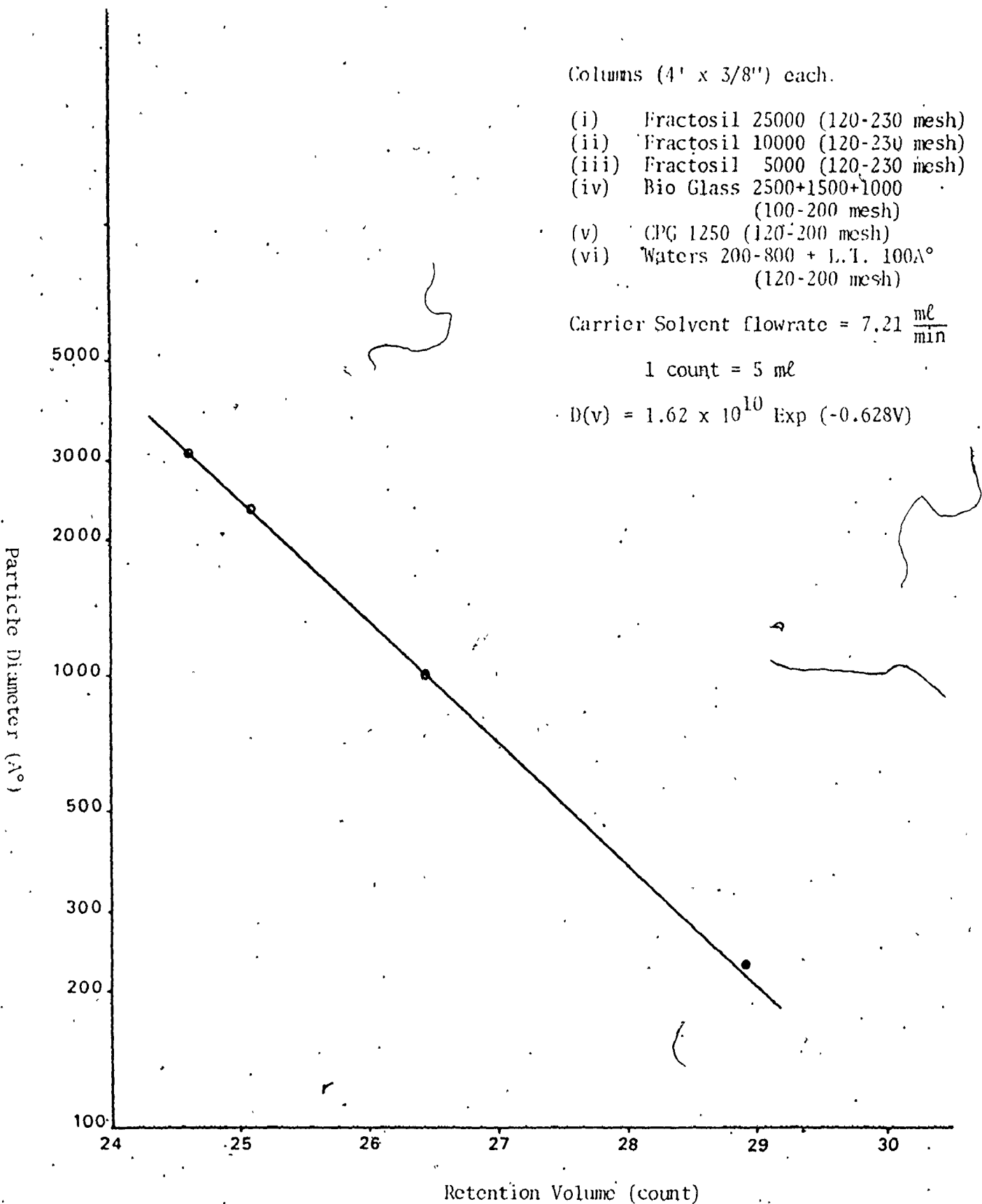


Figure 3: Particle diameter-retention volume calibration curve
o-PS, •-silica

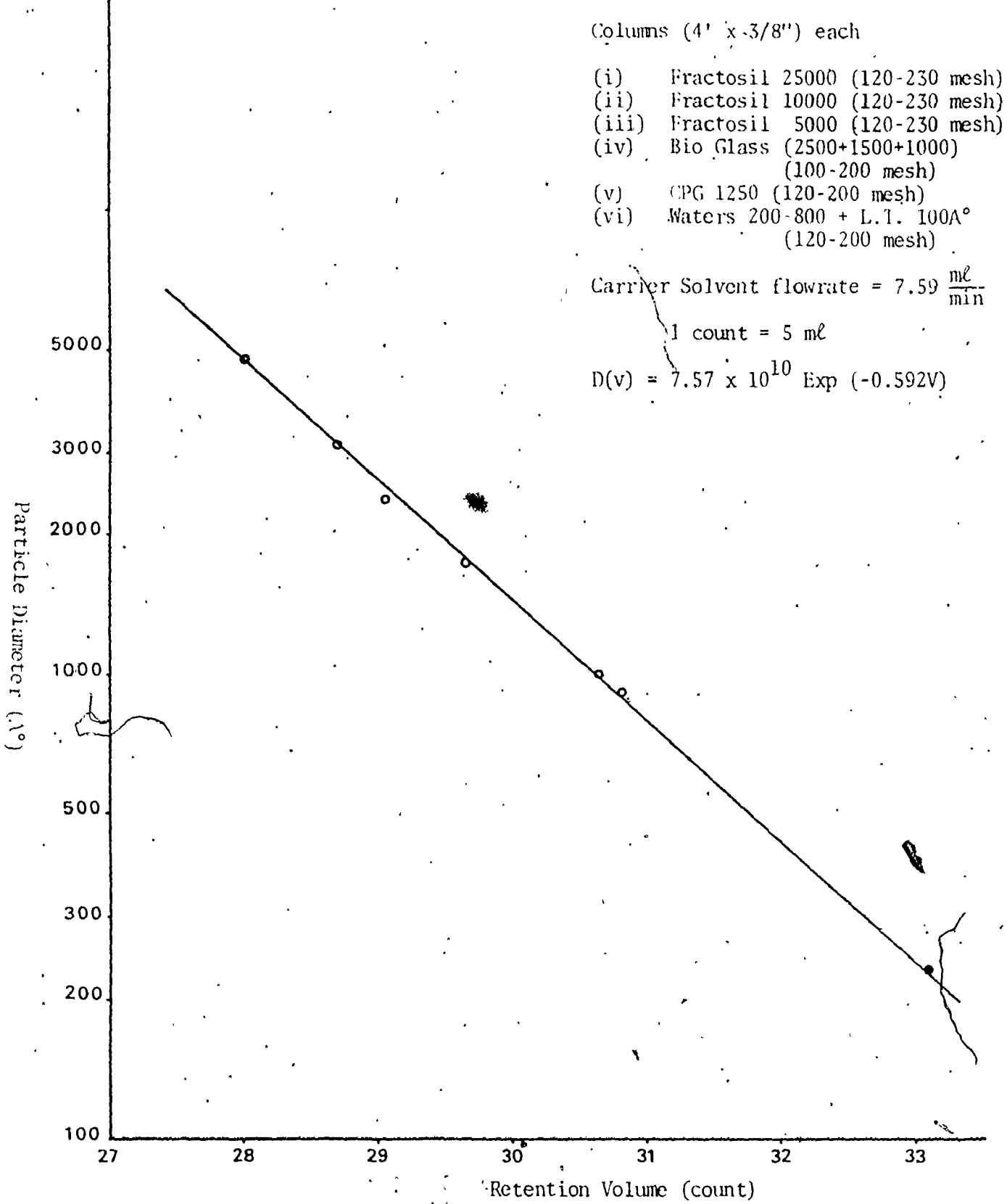


Figure 4: Particle diameter-retention volume calibration curve
○-PS, ●-silica

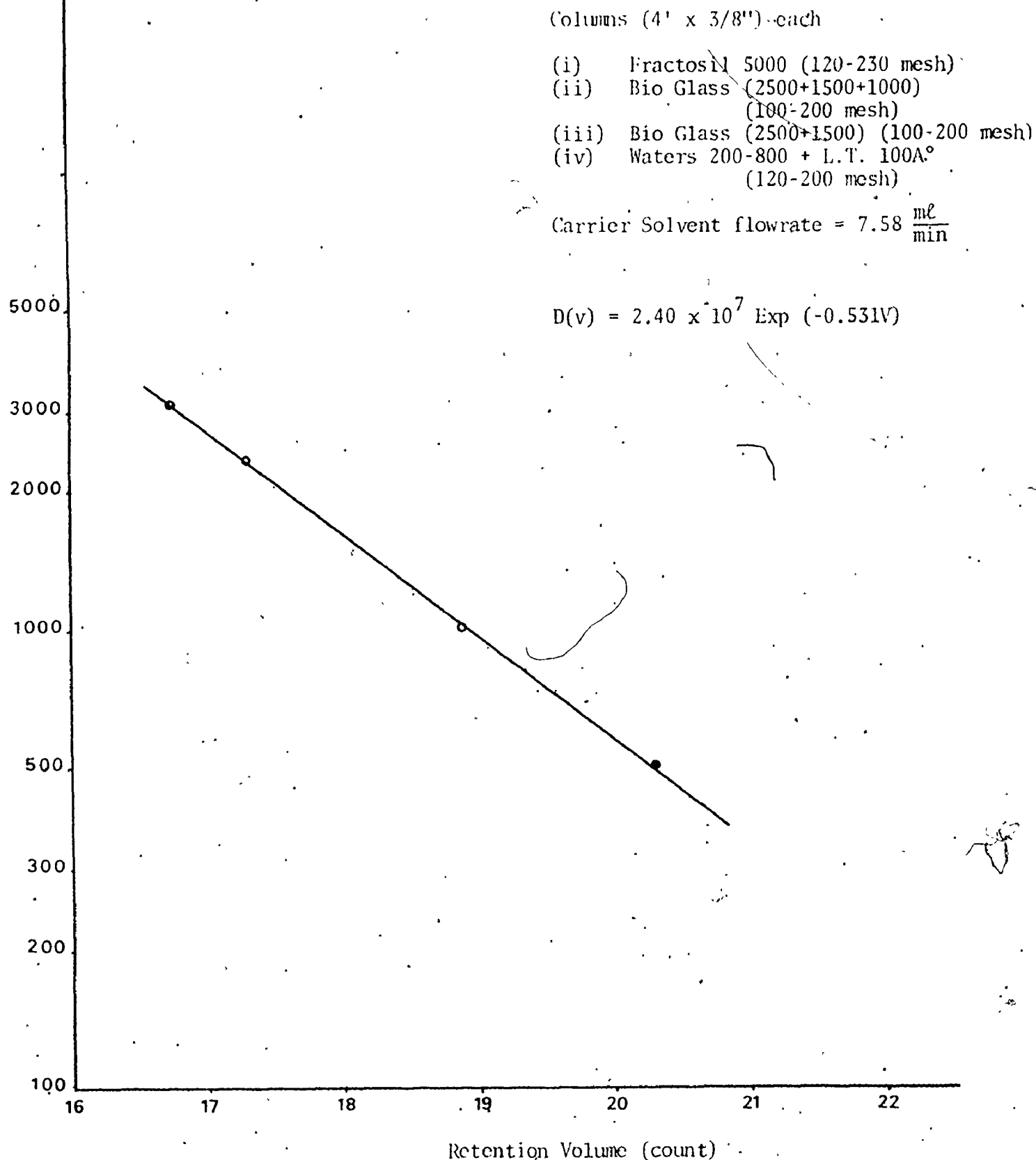


Figure 5: Particle diameter-retention volume calibration curve
○-PS, ●-SMA

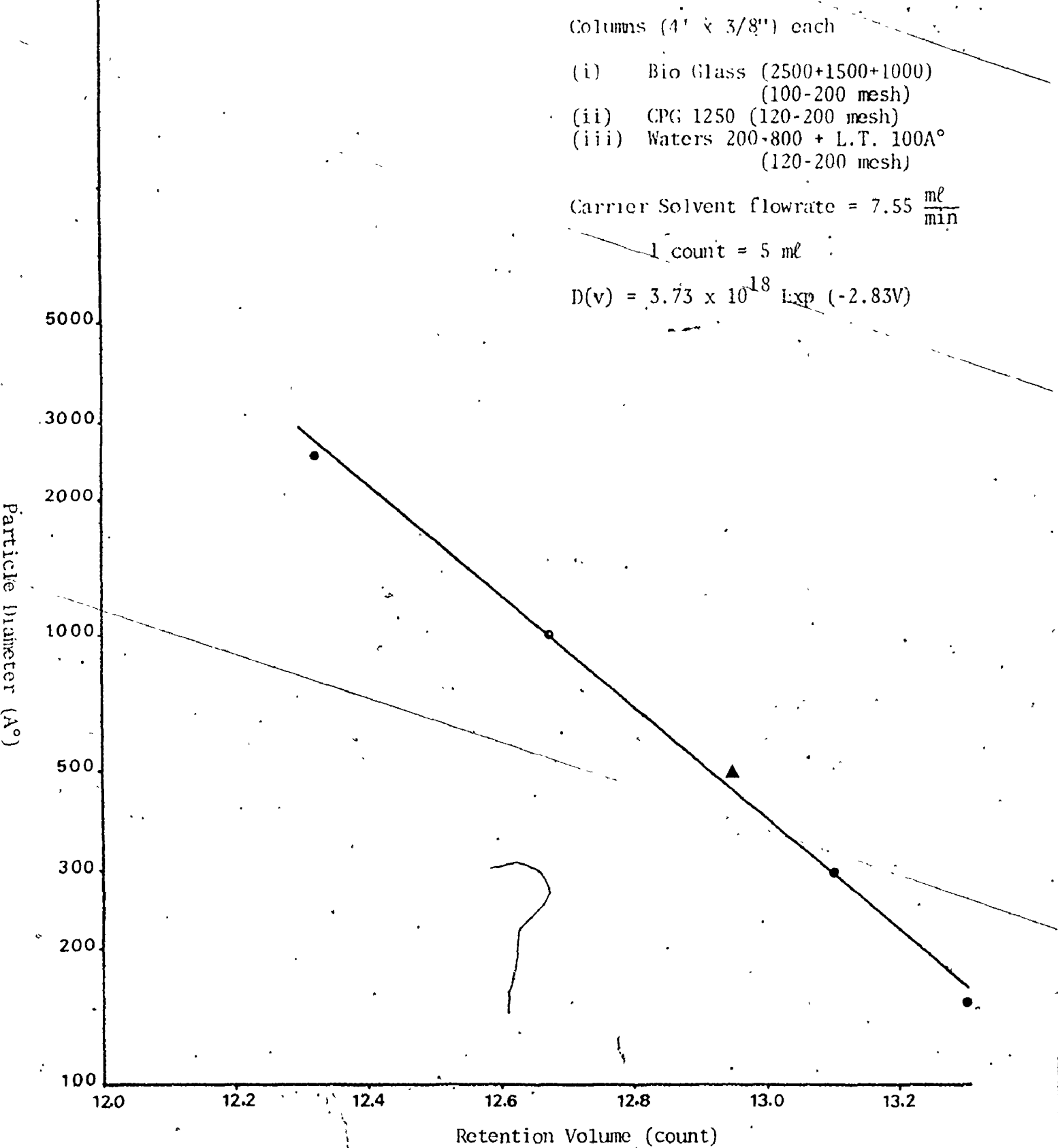


Figure 6: Particle diameter-retention volume calibration curve
○-PS, ▲-SMA, ●-silica

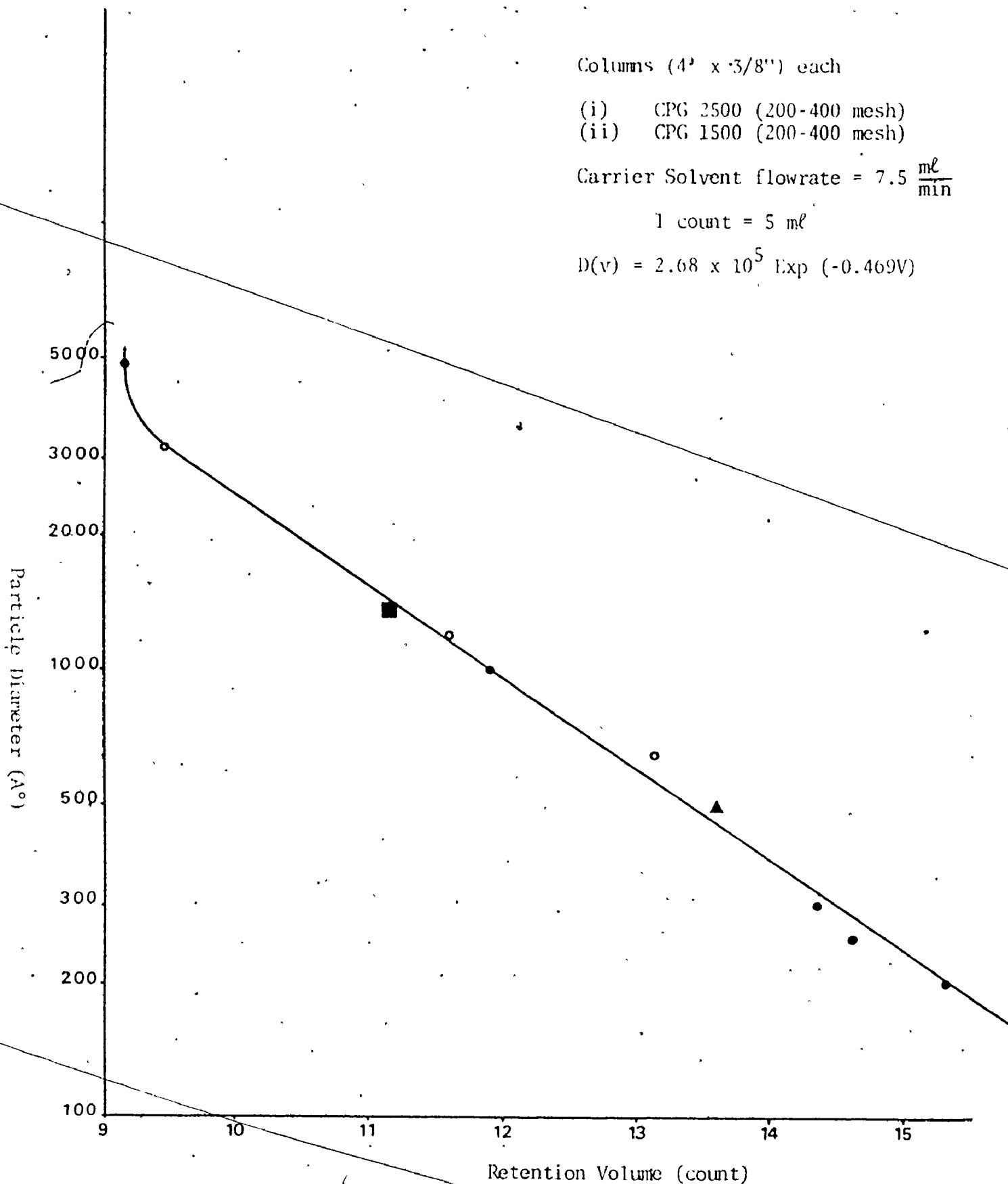


Figure 7: Particle-diameter-retention volume calibration curve
 o-PS, •-silica, ▲-SMA and ■-BD/AN

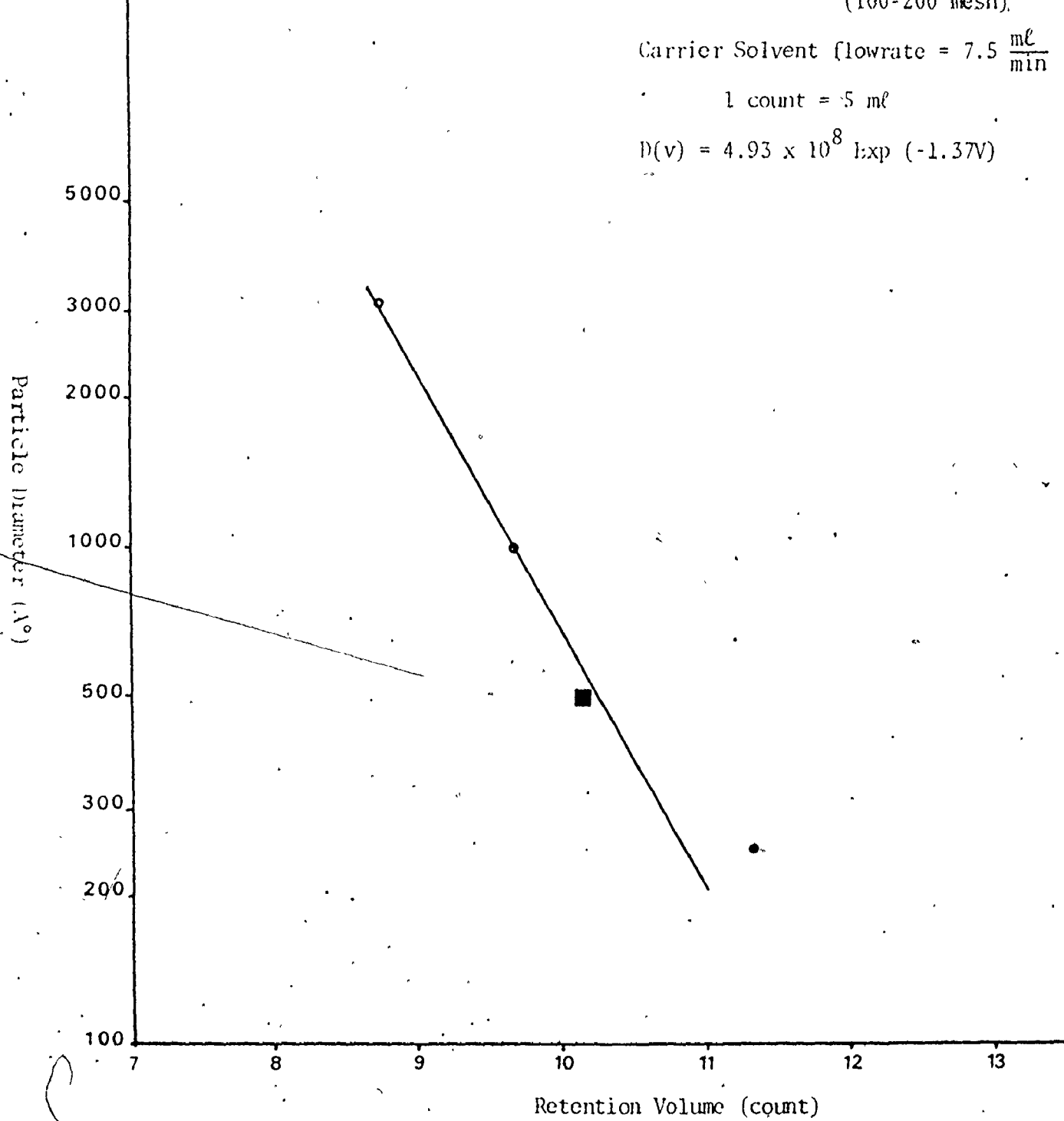


Figure 8: Particle diameter-retention volume calibration curve
○-PS, ■-SMA, ●-Nalco

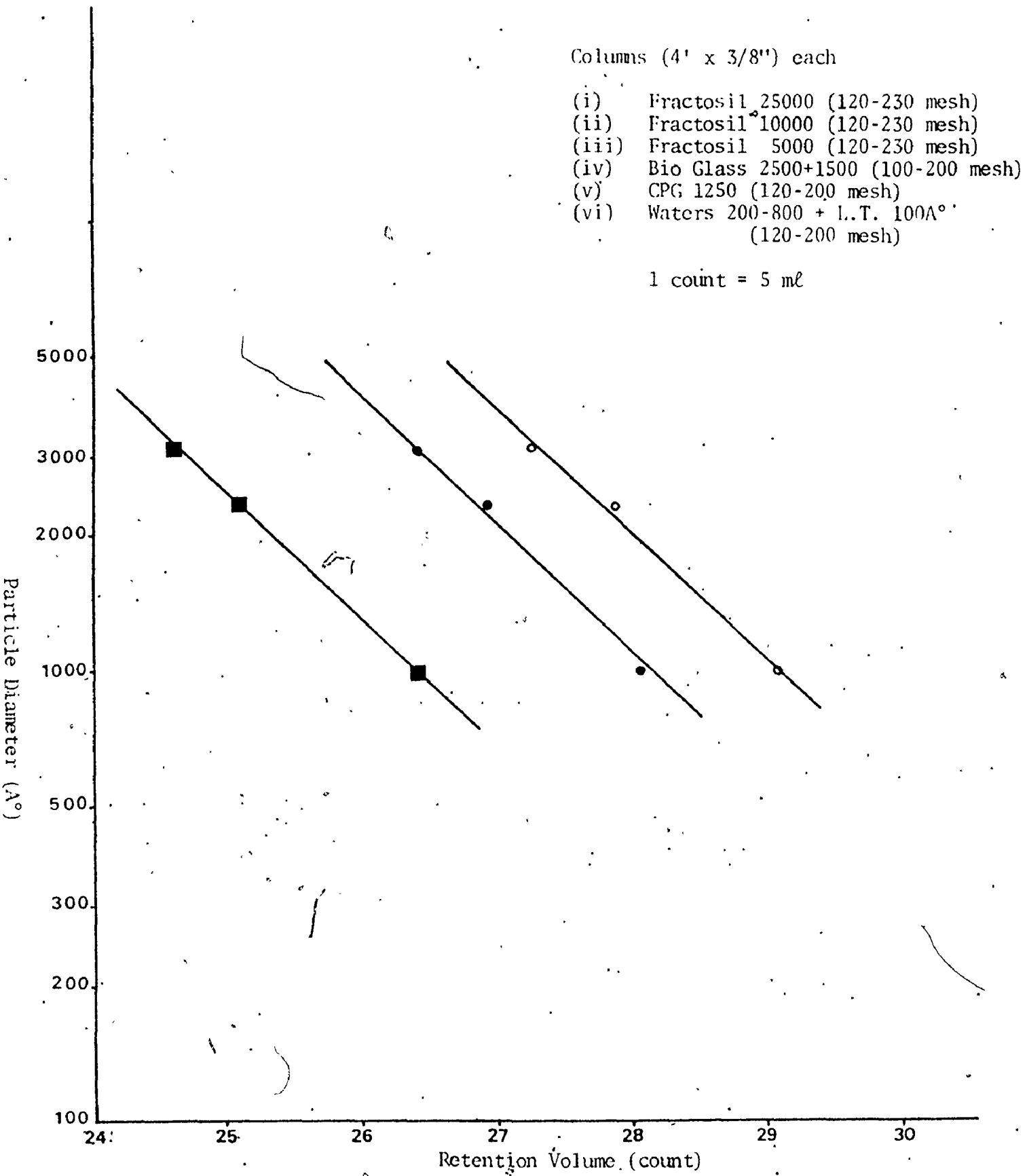


Figure 9: Effect of flowrate on the calibration curve (uncorrected for the error due to the siphon)

○ 0.94 ml/min
 ● 2.58 ml/min
 ■ 7.5 ml/min

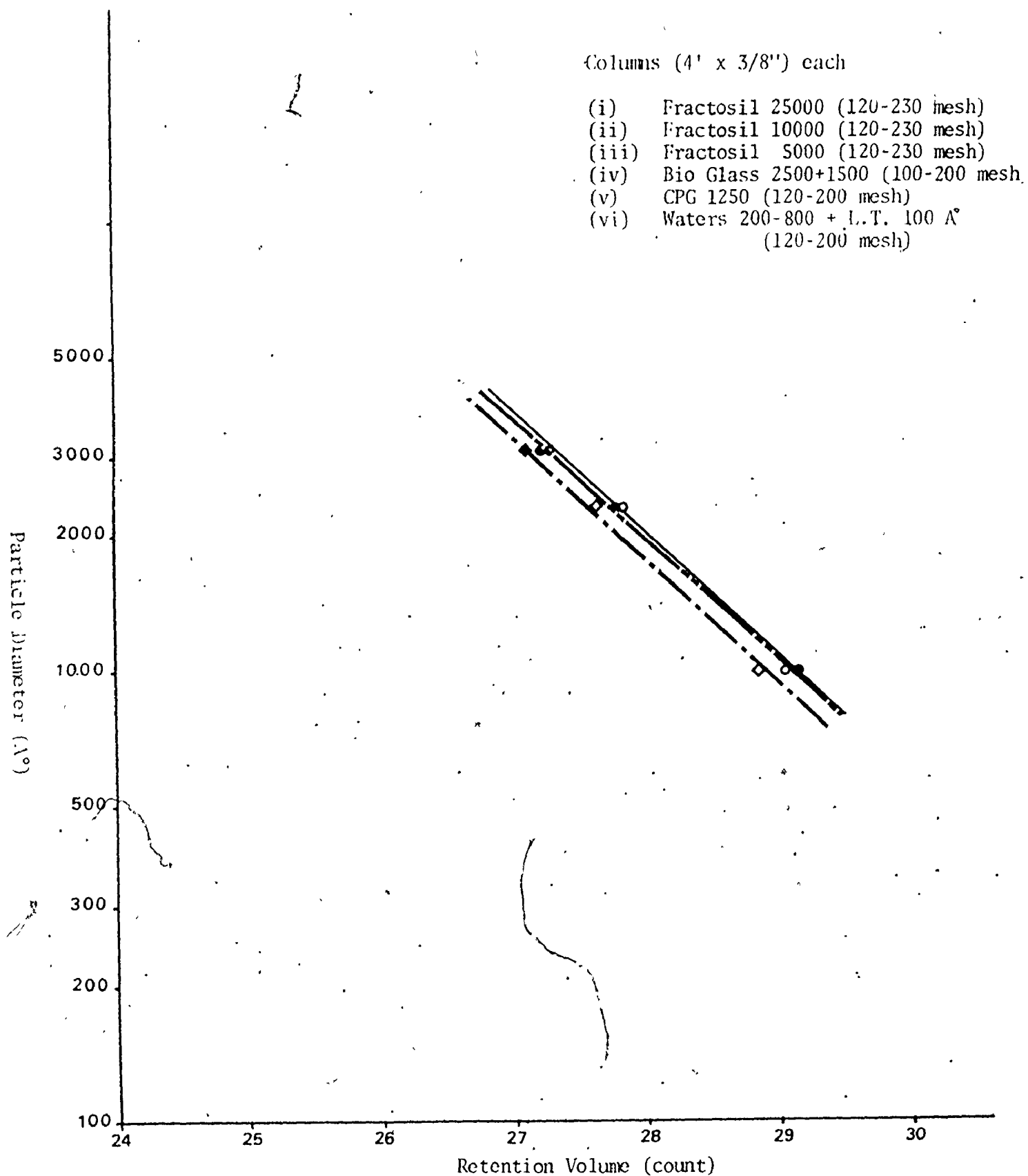


Figure 10: Effect of solvent flowrate on the particle diameter-retention volume calibration curve after correcting the error due to the siphon - —— 0.94 ml/min, - - - 7.5 ml/min, - - - 2.58 ml/min

- (i) Fractosil 10000 (120-230 mesh)
- (ii) Fractosil 5000 (120-230 mesh)
- (iv) Bio Glass (2500+1500) (100-200 mesh)
- (v) CPG 1250 (120-200 mesh)
- (vi) Waters 200-800 + L.T. 100A° (120-200 mesh)

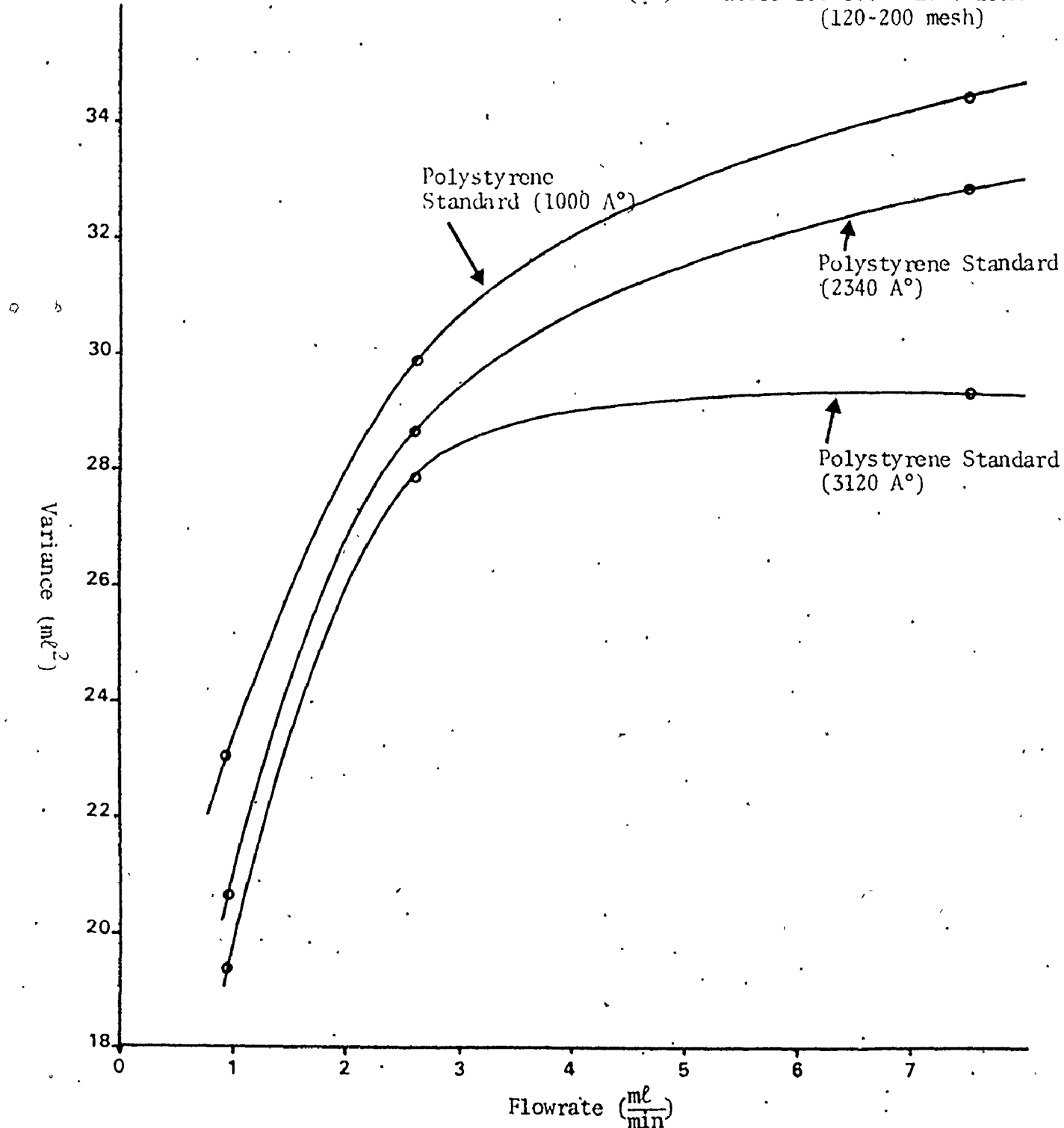


Figure 11: Effect of solvent flowrate on variance

- (i) CPG 2500 (200-400 mesh)
(ii) CPG 1500 (200-400 mesh)

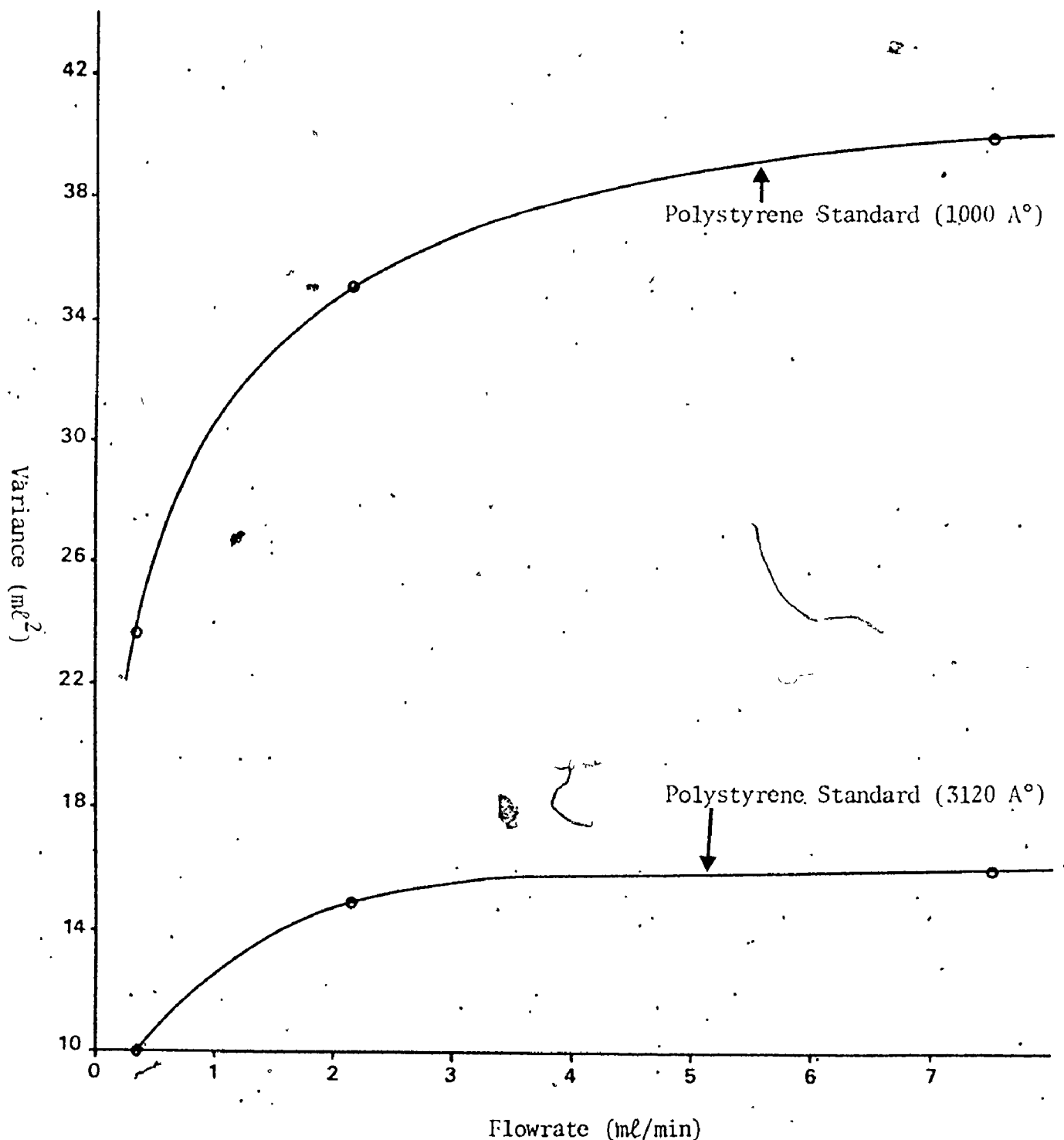


Figure 12: Effect of solvent flowrate on variance

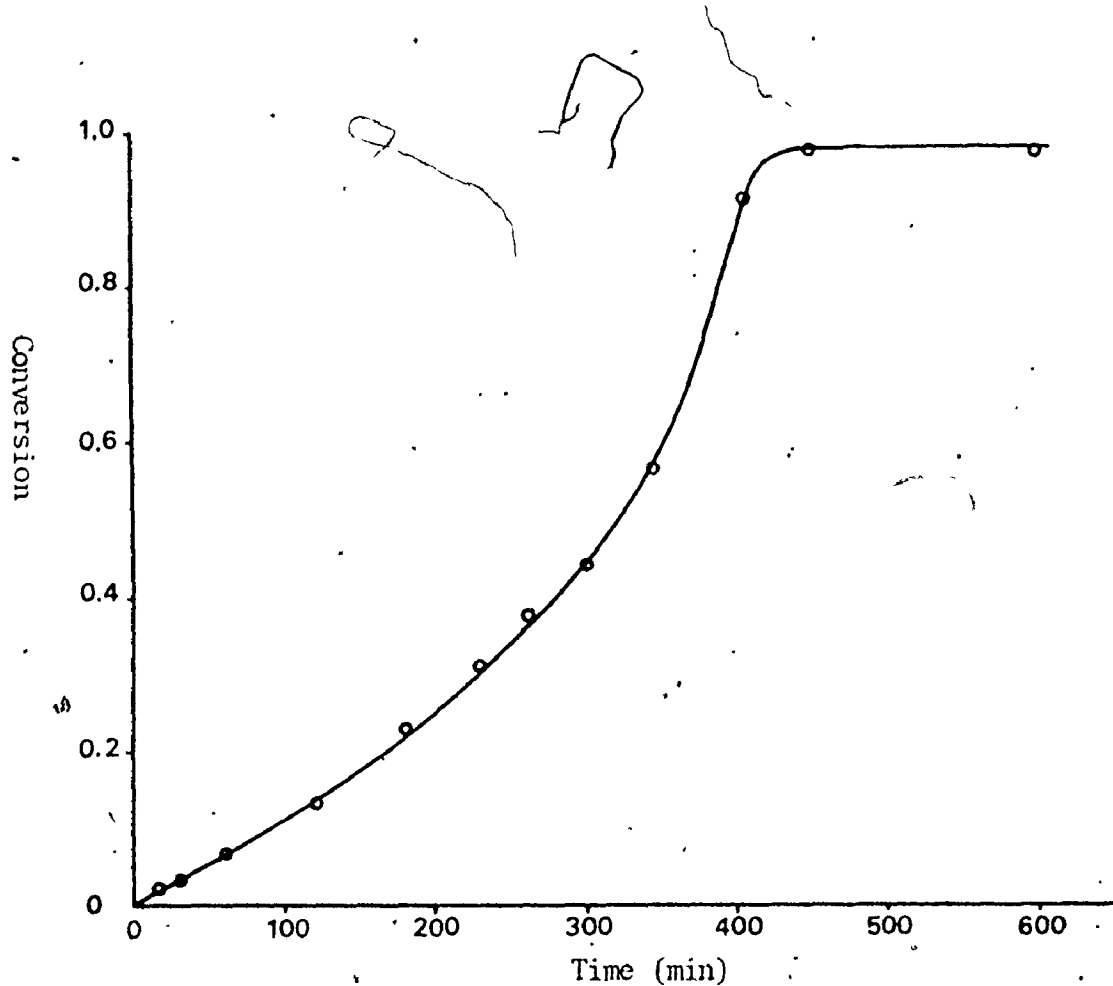


Figure 13(a): Conversion-time history for the surfactant-free emulsion polymerization of styrene at 70.5 °C

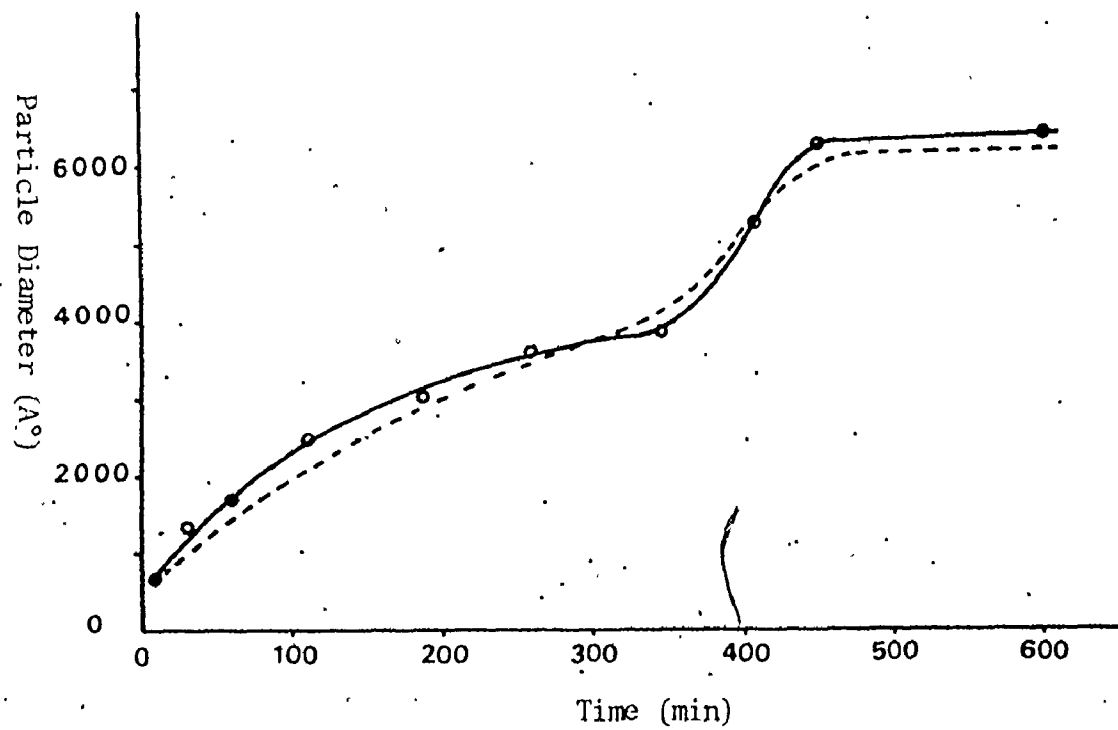


Figure 13(b): Particle diameter-time history for the surfactant-free emulsion polymerization of styrene at 70.5 °C
 o—measured by LEC, --- measured by electron microscope

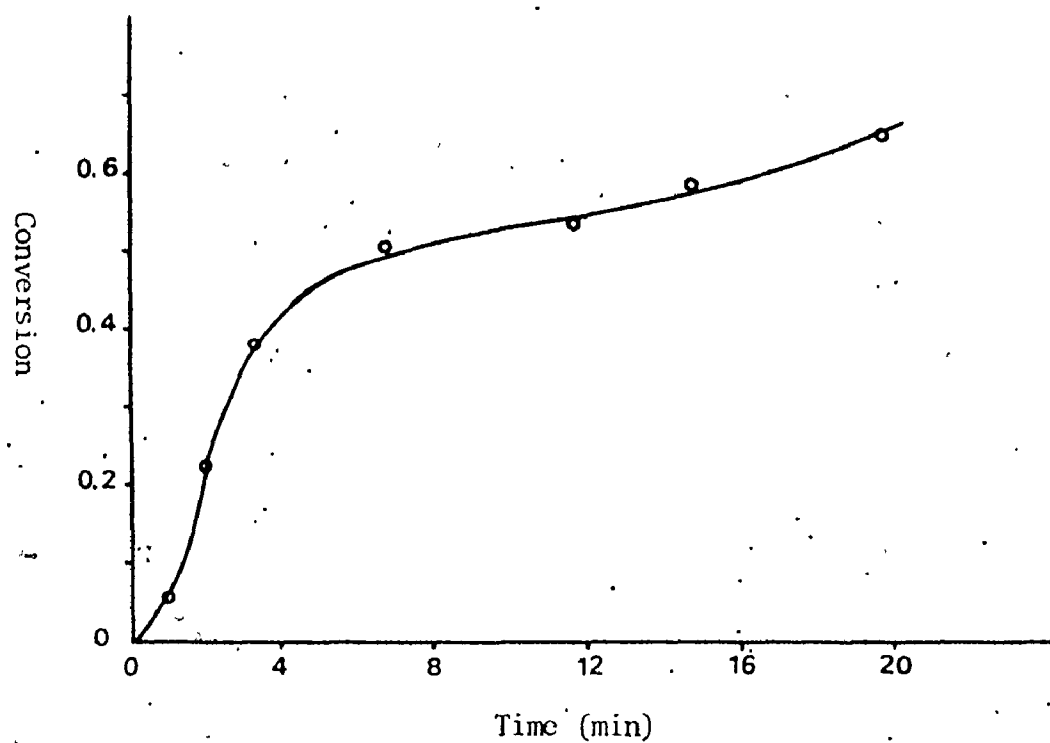


Figure 14(a): Conversion-time history for the surfactant-free emulsion polymerization of vinyl acetate at 85 °C

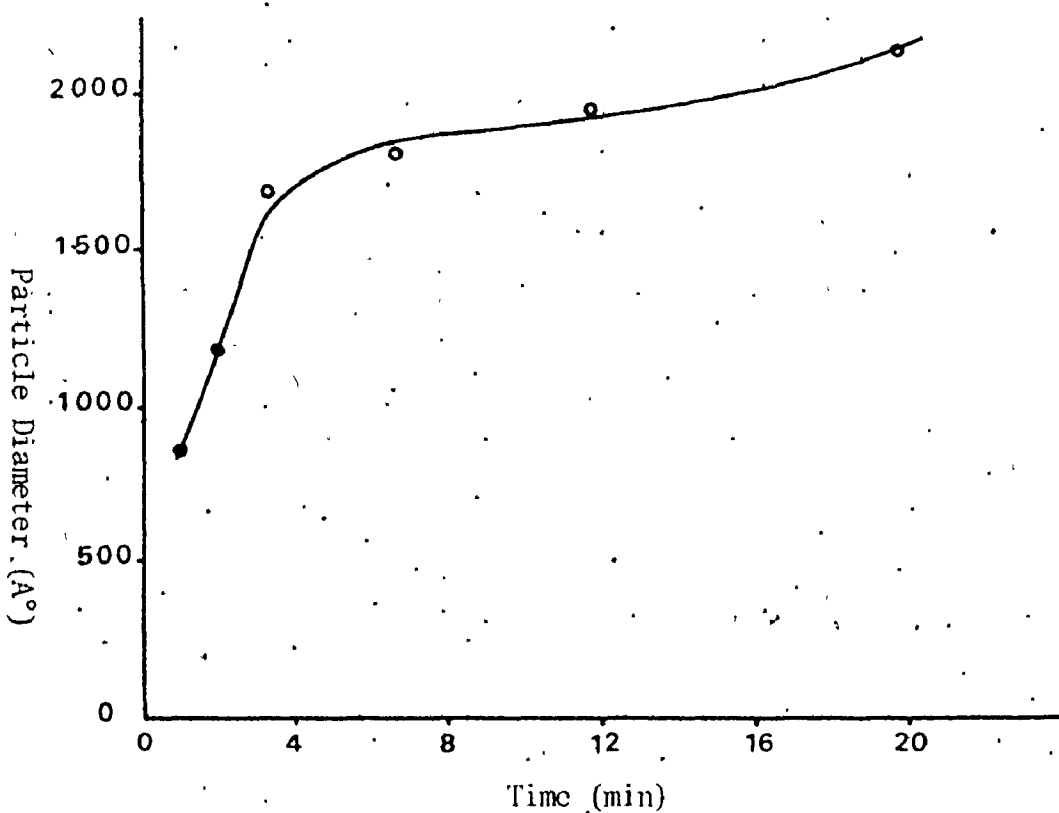


Figure 14(b): Particle diameter-time history for the surfactant-free emulsion polymerization of vinyl acetate at 85 °C

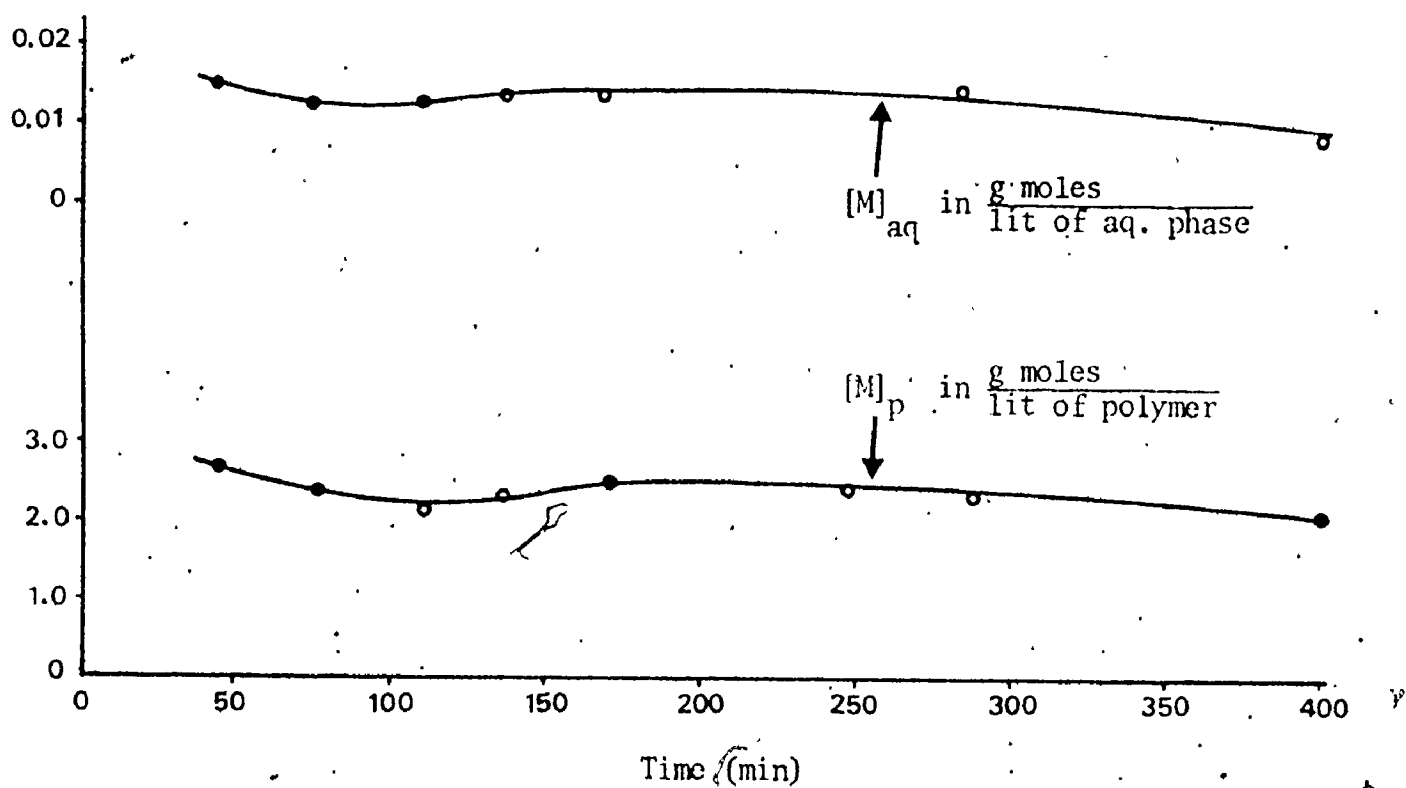


Figure 15(a): Concentration of vinyl acetate in aqueous and in polymer phase vs time for an emulsion polymerization of vinyl acetate with continuous monomer addition

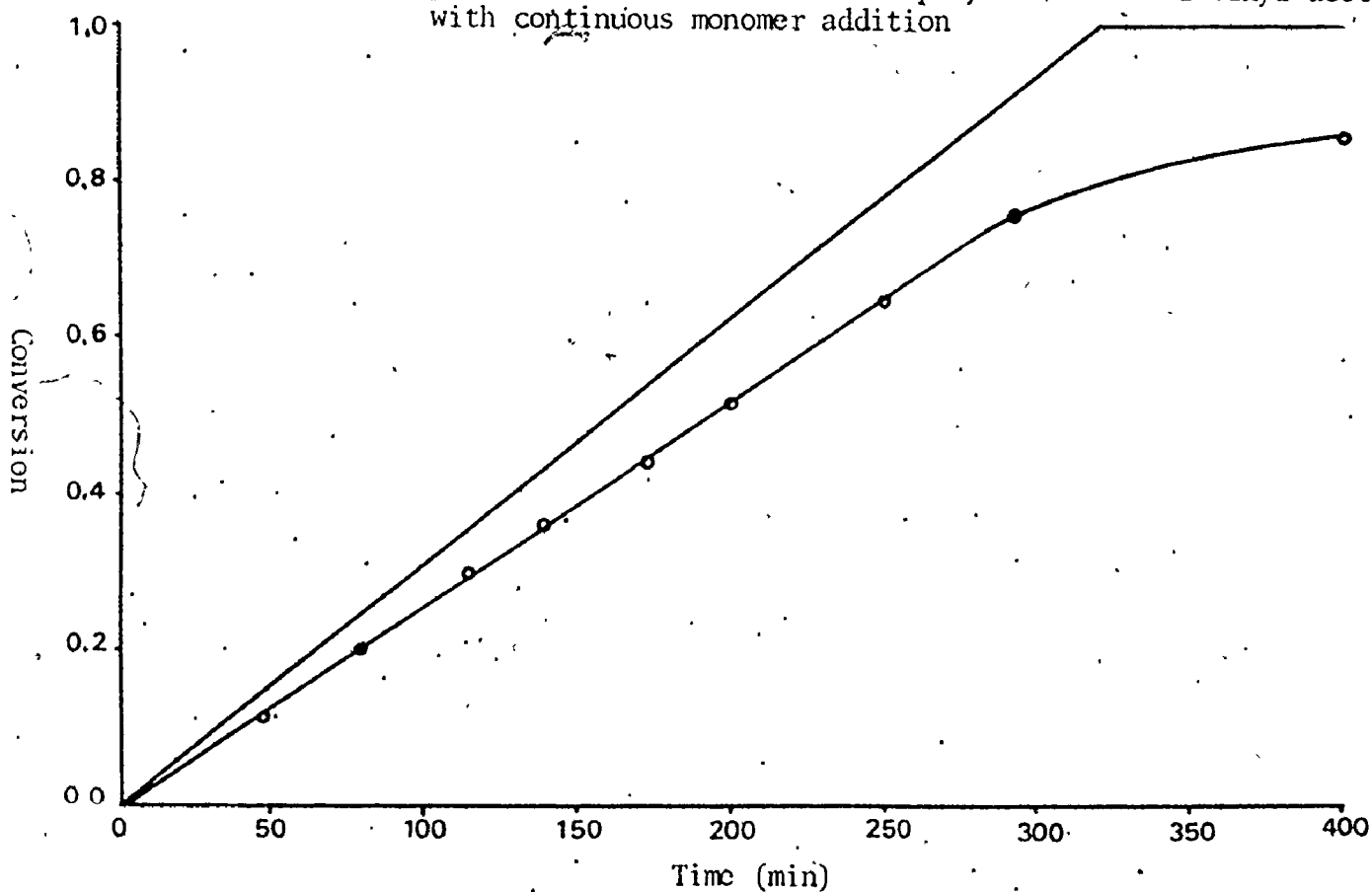


Figure 15(b): Conversion-time history for an emulsion polymerization of vinyl acetate with continuous addition of the monomer

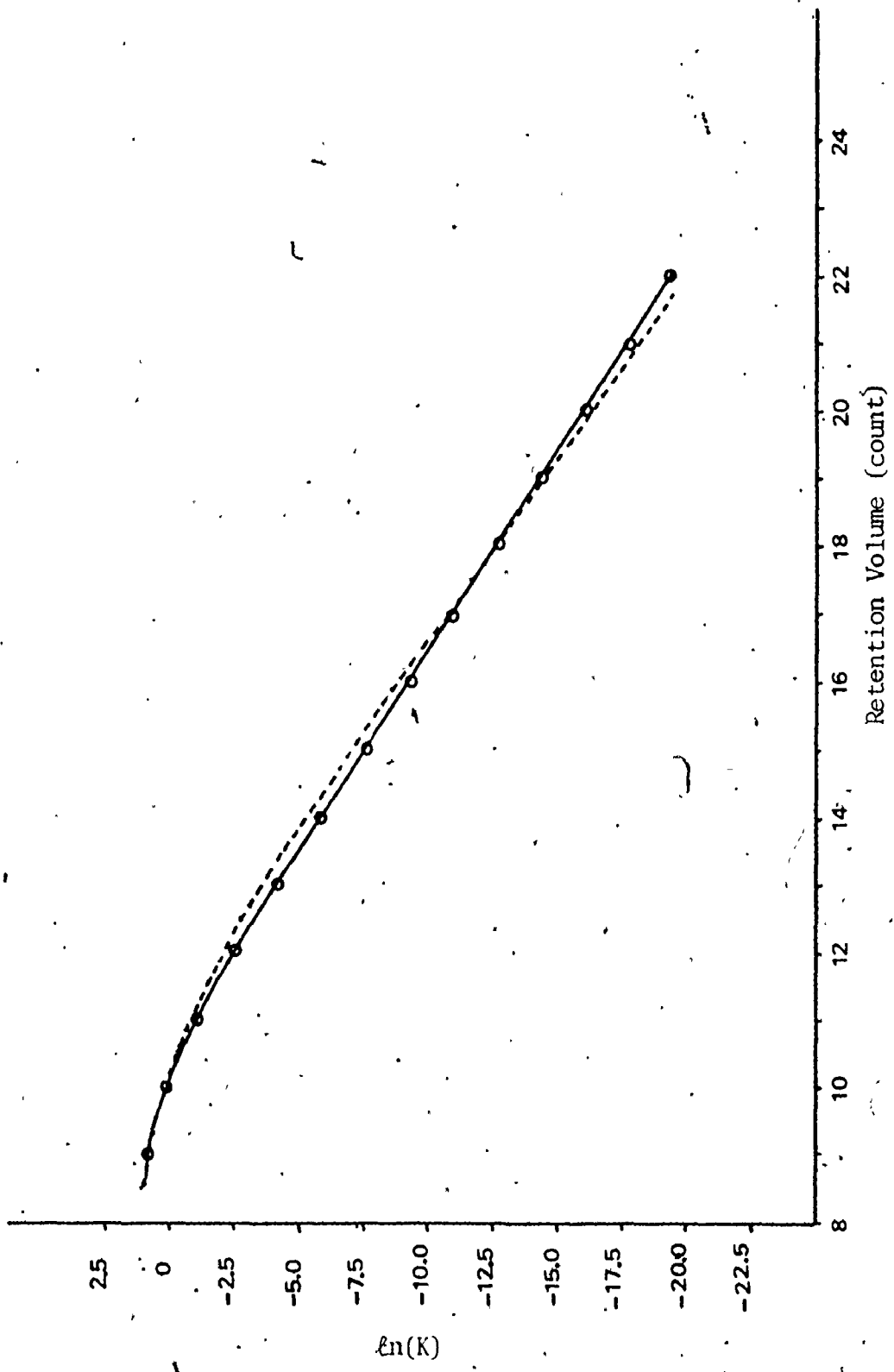


Figure 16: Extinction Coefficient vs. Retention Volume
— calculated from Mie Theory
--- calculated from the sum of exponentials

TABLE I

Correction Factors for Various Diameter Averages for a Turbidity Detector in the Rayleigh Scattering Regime and for a Refractometer with Gaussian Axial Dispersion

| Diameter Average | Correction Factor | |
|------------------|--|--|
| | Turbidity Detector ($\gamma = 6$) | Refractometer ($\gamma = 3$) |
| D_n | $\text{Exp} \left(-\frac{11D^2\sigma^2}{2} \right)$ | $\text{Exp} \left(-\frac{5D^2\sigma^2}{2} \right)$ |
| D_s | $\text{Exp} \left(-\frac{10D^2\sigma^2}{2} \right)$ | $\text{Exp} \left(-\frac{4D^2\sigma^2}{2} \right)$ |
| D_{ss} | $\text{Exp} \left(-\frac{7D^2\sigma^2}{2} \right)$ | $\text{Exp} \left(-\frac{D^2\sigma^2}{2} \right)$ |
| D_w | $\text{Exp} \left(-\frac{5D^2\sigma^2}{2} \right)$ | $\text{Exp} \left(-\frac{D^2\sigma^2}{2} \right)$ |
| D_v | $\text{Exp} \left(-\frac{9D^2\sigma^2}{2} \right)$ | $\text{Exp} \left(-\frac{3D^2\sigma^2}{2} \right)$ |
| D_τ | $\text{Exp} \left(-\frac{3D^2\sigma^2}{2} \right)$ | $\text{Exp} \left(-\frac{-3D^2\sigma^2}{2} \right)$ |

TABLE 2

Axial Dispersion Correction Factors for a General
Detector for an Instrumental Spreading
Function Which Includes a
Term for Skewing

| Diameter Average | Correction Factor |
|------------------|---|
| D_n | $\text{Exp}\left(\frac{(2\gamma-1)D_2^2\sigma^2}{2}\right)\left(\frac{1+\gamma^3\alpha'D_2^3}{1-(1-\gamma)^3\alpha'D_2^3}\right)$ |
| D_s | $\text{Exp}\left(\frac{(2\gamma-2)D_2^2\sigma^2}{2}\right)\left(\frac{1+\gamma^3\alpha'D_2^3}{1-(2-\gamma)^3\alpha'D_2^3}\right)^{1/2}$ |
| D_{ss} | $\text{Exp}\left((2\gamma-5)\frac{D_2^2\sigma^2}{2}\right)\left(\frac{1-(2-\gamma)^3\alpha'D_2^3}{1-(3-\gamma)^3\alpha'D_2^3}\right)$ |
| D_w | $\text{Exp}\left((2\gamma-7)\frac{D_2^2\sigma^2}{2}\right)\left(\frac{1-(3-\gamma)^3\alpha'D_2^3}{1-(4-\gamma)^3\alpha'D_2^3}\right)$ |
| D_v | $\text{Exp}\left((2\gamma-3)\frac{D_2^2\sigma^2}{2}\right)\left(\frac{1+\gamma^3\alpha'D_2^3}{1-(3-\gamma)^3\alpha'D_2^3}\right)^{1/3}$ |
| D_τ | $\text{Exp}\left((2\gamma-9)\frac{D_2^2\sigma^2}{2}\right)\left(\frac{1-(3-\gamma)^3\alpha'D_2^3}{1-(6-\gamma)^3\alpha'D_2^3}\right)^{1/3}$ |

TABLE 3

Column Packing Used for Evaluation of
Liquid Exclusion Chromatography (LEC)

| Packing Type | Mean Pore Diameter (\AA) | Particle Size (mesh) |
|--|-------------------------------------|-------------------------------|
| Fractosil 25,000 (E. Merck, Darmstat) | 30,000 | 120-230 |
| Fractosil 10,000 | 14,000 | 120-230 |
| Fractosil 5,000 | 4,900 | 120-230 |
| CPG-1250 (Corning Glass Works, Corning, New York) | 1,100 | 120-200 |
| CPG-2500 | 2,500 | 200-400 |
| CPG-1500 | 1,500 | 200-400 |
| Bio Glass 2500 (Bio-Rad Laboratories Richmond, California) | 2,500 | 100-200 |
| Bio Glass 1500 | 1,500 | 100-200 |
| Bio Glass 1000 | 1,000 | 100-200 |
| Glass (Water Associates Inc.) | 400-800 200-400 L.T. 100 | 120-200 120-200 120-200 |

TABLE 4

Particle Standards Used for Evaluation
of Liquid Exclusion Chromatography (LEC)

| Particle Type | Diameter (μ) | Source |
|----------------------------------|--------------------|--|
| Polystyrene (Ps) | 1.011 | Union Carbide Corp., South Charleston, West Virginia |
| | 0.760 | |
| | 0.481 | |
| | 0.312 | Dow Chemical Company, Midland, Michigan |
| | 0.234 | |
| | 0.100 | Polysciences Inc., Rydal, Pennsylvania |
| Styrene-Methacrylic Acid Polymer | 0.091 | E.F. Fullam Inc. |
| | 0.050 | Eastman Kodak, Rochester, New York |
| Silica Sol | 0.250 | E.I. DuPont DeNemours & Co., Wilmington, Delaware |
| | 0.1-0.14 | |
| | 0.05-0.08 | |
| | 0.025-0.035 | |
| Ludox TM | 0.010-0.020 | Nalco Chemical Co., Chicago |
| Ludox HS | 0.010-0.020 | |
| Ludox SM | 0.022-0.025 | Sohio, Cleveland, Ohio |
| Silica (Nalco) | 0.023 | |

TABLE 5

Values of $(D_2^2 \sigma^2)$ for Polystyrene Standard (1000 Å°)
with Different Column Combinations

| Columns | Refer | $D_2^2 \sigma^2$ |
|------------------|----------|------------------|
| A, B, C, D, E, F | Figure 2 | 0.57 |
| A, B, C, D, E, F | Figure 3 | 0.54 |
| A, B, C, D, E, F | Figure 4 | 0.59 |
| C, D, G, F | Figure 5 | 0.32 |
| D, E, F | Figure 6 | 3.04 |
| H, I | Figure 7 | 0.25 |
| D, G | Figure 8 | 1.19 |

In the above tables the following abbreviations were used:

| | |
|----------|---|
| | Packing material |
| Column A | Fractosil 25,000 (120-230 mesh) |
| Column B | Fractosil 10,000 (120-230 mesh) |
| Column C | Fractosil 5,000 (120-230 mesh) |
| Column D | Bio Glass (2500+1500+1000) (100-200 mesh) |
| Column E | CPG 1250 (120-200 mesh) |
| Column F | Waters 200-800+L.T. 100A° (120-200 mesh) |
| Column G | Bio Glass (2500+1500) (100-200 mesh) |
| Column H | CPG 2500 (200-400 mesh) |
| Column I | CPG 1500 (200-400 mesh) |

TABLE 6
Effect of Solvent Flowrate on the Variance
of Polystyrene Standard (1000 Å°)

| Flowrate (mℓ/min) | Variance * (mℓ ²) |
|----------------------|----------------------------------|
| 0.94 | 23.09 |
| 2.58 | 29.75 |
| 7.50 | 34.47 |

* measured using raw chromatogram uncorrected
for axial dispersion and Gaussian distribution

Columns (4' x 3/8") each

- (i) Fractosil 25,000 (120-230 mesh)
- (ii) Fractosil 10,000 (120-230 mesh)
- (iii) Fractosil 5,000 (120-230 mesh)
- (iv) Bio Glass (2500+1500) (100-200 mesh)
- (v) CPG 1250 (120-200 mesh)
- (vi) Waters 200-800 + L.T. 100 (120-200 mesh)

1 count = 5 mℓ

TABLE 7
Effect of Solvent Flowrate on the Variance
of Polystyrene Standard (2340 \AA°)

| Flowrate (ml/min) | Variance * (ml ²) |
|----------------------|----------------------------------|
| 0.94 | 20.66 |
| 2.58 | 28.69 |
| 7.50 | 32.89 |

* measured using raw chromatogram uncorrected
for axial dispersion and Gaussian distribution

Columns (4" x 3/8") each

- (i) Fractosil 25,000 (120-230 mesh)
- (ii) Fractosil 10,000. (120-230 mesh)
- (iii) Fractosil 5,000 (120-230 mesh)
- (iv) Bio Glass (2500+1500) (100-200 mesh)
- (v) CPG 1250 (120-200 mesh)
- (vi) Waters 200-800 + L.T. <100 (120-200 mesh)

1 count = 5 ml

TABLE 8
Effect of Solvent Flowrate on the Variance
of Polystyrene Standard (3120 Å°)

| Flowrate (mℓ/min.) | Variance * (mℓ ²) |
|-----------------------|----------------------------------|
| 0.94 | 19.39 |
| 2.58 | 27.88 |
| 7.50 | 29.34 |

* measured using raw chromatogram uncorrected
for axial dispersion and Gaussian distribution

Columns (4' x 3/8") each

- (i) Fractosil 25,000 (120-230 mesh)
- (ii) Fractosil 10,000 (120-230 mesh)
- (iii) Fractosil 5,000 (120-230 mesh)
- (iv) Bio Glass (2500+1500) (100-200 mesh)
- (v) CPG 1250 (120-200 mesh)
- (vi) Waters 200-800 + L.T. 100 (120-200 mesh)

1 count = 5 mℓ

TABLE 9
Effect of Solvent Flowrate on the Variance
of Polystyrene Standard (3120 Å°)

| Flowrate (ml/min) | Variance * (ml ²) |
|----------------------|----------------------------------|
| 0.33 | 10.05 |
| 2.14 | 14.91 |
| 7.50 | 15.98 |

* measured using raw chromatogram uncorrected
for axial dispersion and Gaussian distribution

Columns (4' x 3/8") each

- (i) CPG 2500 (200-400 mesh)
- (ii) CPG 1500 (200-400 mesh)

1 count = 5 ml

TABLE 10

Effect of Solvent Flowrate on the Variance
of Polystyrene Standard (1000 Å°)

| Flowrate (m /min) | Variance * (m ²) |
|----------------------|---------------------------------|
| 0.33 | 23.75 |
| 2.14 | 35.16 |
| 7.50 | 40.09 |

* measured using raw chromatogram uncorrected
for axial dispersion and Gaussian distribution

Column (4' x 3/8") each

- (i) CPG 2500 (200-400 mesh)
- (ii) CPG 1500 (200-400 mesh)

TABLE 11
Reproducibility of Peak Position and Variance of
Polystyrene Standard (1000 Å°)

| Flowrate (mℓ/min) | Peak Position (count) | Diameter (Å°) | Variance * (mℓ ²) |
|----------------------|--------------------------|------------------|----------------------------------|
| 7.5 | 29.32 | 988 | 31.88 |
| | 29.28 | 1012 | 35.94 |
| | 29.30 | 1000 | 33.97 |
| | 29.28 | 1012 | 35.36 |
| | 29.28 | 1012 | 34.76 |
| Mean | 29.29 | 1005 | 34.38 |
| Std. Dev. | 0.018 | 10.7 | 1.58 |
| % Std. Dev. | 0.06 | 1.06 | 4.59 |

* measured using raw chromatogram uncorrected for axial dispersion and Gaussian distribution

Columns (4' x 3/8") each

- (i) Fractosil 25,000 (120-230 mesh)
- (ii) Fractosil 10,000 (120-230 mesh)
- (iii) Fractosil 5,000 (120-230 mesh)
- (iv) Bio Glass (2500+1500) (100-200 mesh)
- (v) CPG 1250 (120-200 mesh)
- (vi) Waters 200-800 + L.T. 100 (120-200 mesh)

1 count = 5 mℓ

TABLE 12

Different Diameter Averages for Polystyrene Standard (1000 Å°)
 Corrected for Axial Dispersion Using Analytical Solution
 with Mie Theory $\sigma^2 = 1.16 \text{ count}^2$, $\alpha' = 0.0$ and
 $D_2 = 0.464 \text{ counts}^{-1}$ (σ^2 measured
 using raw chromatogram)

| | D_n | D_s | D_{ss} | D_w | D_v | D_τ |
|---------|-------|-------|----------|-------|-------|----------|
| 1st run | 791 | 742 | 667 | 711 | 716 | 811 |
| 2nd run | 879 | 825 | 746 | 793 | 798 | 885 |
| 3rd run | 924 | 877 | 810 | 848 | 854 | 926 |
| 4th run | 551 | 519 | 496 | 611 | 511 | 790 |
| 5th run | 712 | 692 | 708 | 806 | 697 | 908 |

| | | | | | | |
|------------|------|------|------|------|------|------|
| Mean | 771 | 731 | 685 | 754 | 715 | 864 |
| Std.Dev. | 148 | 138 | 118 | 94 | 130 | 60.2 |
| % Std.Dev. | 19.2 | 18.9 | 17.3 | 12.5 | 16.0 | 6.9 |

TABLE 13

Different Diameter Averages for Polystyrene Standard (3120 \AA°)
 Corrected for Axial Dispersion using Analytical Solution
 $\sigma^2 = 1.029 \text{ count}^2$, and $D_2 = 0.468 \text{ counts}^{-1}$ (σ^2 measured
 using raw chromatogram)

| Diameter Average | Uncorrected Diameter Averages | | Corrected Diameter Averages | | |
|------------------|-------------------------------|----------------|-------------------------------------|--------------|---------------------------------|
| | Rayleigh Scattering | Mie Scattering | Rayleigh Scattering $\alpha=0.0$ | $\alpha=1.5$ | Mie Scattering $\alpha'=0.0$ |
| D_n | 212 | 214 | 731 | 1237 | 617 |
| D_s | 220 | 226 | 678 | 1204 | 612 |
| D_{ss} | 263 | 330 | 577 | 1214 | 826 |
| D_w | 371 | 861 | 650 | 1501 | 1526 |
| D_v | 234 | 256 | 642 | 1075 | 676 |
| D_t | 810 | 1843 | 1135 | 3183 | 1942 |

TABLE 14
 Different Diameter Averages for Polystyrene Standard (1000 Å)
 Corrected for Axial Dispersion using Analytical Solution
 $\sigma_2 = 1.16$ count², $\sigma_1 = 0.0$ and $D_2 = 0.464$ counts⁻¹
 $(\sigma_2$ measured using raw chromatogram)

| Diameter Average | Uncorrected Diameter Averages | | Corrected Diameter Averages | |
|------------------|-------------------------------|-----------------------------------|---|----------------|
| | Rayleigh Scattering | Mie Scattering Using Coefficients | Rayleigh Scattering Using the Exponential Fit | Mie Scattering |
| D_n | 200 | 203 | 220 | 791 |
| D_s | 213 | 219 | 242 | 742 |
| D_{ss} | 278 | 308 | 360 | 667 |
| D_w | 381 | 476 | 532 | 711 |
| D_v | 233 | 245 | 276 | 716 |
| D_t | 558 | 801 | 813 | 694 |
| | | | | 902 |

TABLE 15

Different Diameter Averages for Standard Nalco (250 Å°)
 Corrected for Axial Dispersion Using Analytical
 Solution $\sigma^2 = 1.69 \text{ count}^2$, $\alpha' = 0.0$ and $D_2 = 0.473 \text{ counts}^{-1}$
 $(\sigma^2 \text{ measured using raw chromatogram})$

| Diameter Average | Uncorrected Diameter Averages | | Corrected Diameter Averages | |
|------------------|-------------------------------|----------------|-----------------------------|----------------|
| | Rayleigh Scattering | Mie Scattering | Rayleigh Scattering | Mie Scattering |
| D_n | 57 | 57 | 451 | 309 |
| D_s | 59 | 59 | 392 | 281 |
| D_{ss} | 73 | 73 | 272 | 234 |
| D_w | 93 | 94 | 239 | 237 |
| D_v | 63 | 64 | 347 | 265 |
| D_x | 136 | 140 | 239 | 247 |

TABLE 16

Different Diameter Averages* for Samples with Known Polydispersity
 Corrected for Axial Dispersion Using Analytical Solution with Mie Theory,
 $\alpha' = 0.0$ and $D_2 = 0.464 \text{ counts}^{-1}$

| Sample | D_n | D_s | D_{ss} | D_w | D_v | D_τ |
|---|-------------|-------------|-------------|--------------|-------------|--------------|
| SMA + Nalco $D_n = 255$ $D_w = 285$ $\sigma^2 = 1.39 \text{ count}^2$ | 230 (52) | 217 (55) | 216 (72) | 279 (110) | 217 (61) | 359 (210) |
| PS(1000) + Nalco $D_n = 250$ $D_w = 272$ $\sigma^2 = 1.25 \text{ count}^2$ | 201 (45) | 182 (46) | 167 (55) | 279 (88) | 177 (49) | 523 (306) |
| PS(1000) + Nalco $D_n = 250$ $D_w = 278$ $\sigma^2 = 1.25 \text{ count}^2$ | 242 (63) | 232 (67) | 255 (89) | 403 (159) | 240 (73) | 620 (418) |
| PS(1000) + Nalco $D_n = 250$ $D_w = 260$ $\sigma^2 = 1.25 \text{ count}^2$ | 281 (45) | 250 (47) | 222 (58) | 336 (98) | 240 (50) | 538 (308) |

* numbers in the brackets represent the respective uncorrected values

TABLE 17

Measured Variances of LEC Chromatograms for the
Surfactant-Free Emulsion Polymerization
of Styrene at 70.5 °C*

| Reaction Time (min) | Particle Diameter (\AA) | Variance ($\text{m}\ell^2$) |
|------------------------|---------------------------------------|----------------------------------|
| 10 | 645 | 33.3 |
| 120 | 2480 | 31.6 |
| 705 | 6430 | 25.9 |

* Polystyrene standard with diameter 0.312μ had a variance of $26.3 \text{ m}\ell^2$ and that with diameter 0.10μ had a variance of $33.3 \text{ m}\ell^2$

TABLE 18

Measured Variances of LEC Chromatograms for the
Surfactant-Free Emulsion Polymerization
of Vinyl Acetate at 85 °C*

| Reaction Time (min) | Particle Diameter (\AA) | Variance ($\text{m}\ell^2$) |
|------------------------|---------------------------------------|----------------------------------|
| 1 | 870 | 49.4 |
| 3.5 | 1710 | 48.5 |
| 7 | 1800 | 52.2 |
| 12 | 1950 | 49.2 |
| 20 | 2020 | 50.1 |

* Polystyrene standard with diameter 0.312μ had a variance of $26.3 \text{ m}\ell^2$ and with diameter 0.10μ had a variance of $33.3 \text{ m}\ell^2$

TABLE 19

Normalized Heights of the Chromatogram for
a Polystyrene Latex Sample at Two Different
Wavelengths Using a Turbidity Detector

| Count | Normalized Height at $\lambda = 254 \text{ nm}$ | Normalized Height at $\lambda = 405 \text{ nm}$ |
|-------|--|--|
| 7.0 | 0 | 0 |
| 7.5 | 0.0002 | 0.0004 |
| 8.0 | 0.0006 | 0.0008 |
| 8.5 | 0.00098 | 0.0013 |
| 9.0 | 0.0014 | 0.0022 |
| 9.5 | 0.0023 | 0.0039 |
| 10.0 | 0.0039 | 0.0060 |
| 10.5 | 0.0072 | 0.0086 |
| 11.0 | 0.0133 | 0.0143 |
| 11.5 | 0.0221 | 0.0207 |
| 12.0 | 0.0292 | 0.0285 |
| 12.5 | 0.0329 | 0.0311 |
| 13.0 | 0.0317 | 0.0307 |
| 13.5 | 0.0264 | 0.0259 |
| 14.0 | 0.0203 | 0.0194 |
| 14.5 | 0.01390 | 0.0138 |
| 15.0 | 0.0099 | 0.0095 |
| 15.5 | 0.0066 | 0.0065 |
| 16.0 | 0.0047 | 0.0047 |
| 16.5 | 0.0033 | 0.0030 |
| 17.0 | 0.0025 | 0.0022 |
| 17.5 | 0.0018 | 0.0017 |
| 18.0 | 0.0014 | 0.0013 |
| 18.5 | 0.0009 | 0.0008 |
| 19.0 | 0.0006 | 0.0004 |
| 19.5 | 0.0002 | 0.0004 |
| 20.0 | 0 | 0 |

TABLE 20

Corrected Diameter* Averages for a Polystyrene Sample Whose Chromatograms were Obtained at Two Different Wavelengths Using a Turbidity Detector

| Diameter Average | $\lambda = 2540 \text{ \AA}^\circ$ | $\lambda = 4050 \text{ \AA}^\circ$ | % Deviation |
|------------------|------------------------------------|------------------------------------|-------------|
| D_n | 289 | 274 | 5.1 |
| D_s | 266 | 246 | 7.5 |
| D_{ss} | 251 | 210 | 16.3 |
| D_w | 380 | 300 | 21.0 |
| D_v | 261 | 233 | 10.7 |
| D_τ | 645 | 590 | 8.5 |

* Diameter averages were corrected with Mie Theory

REFERENCES 8

1. M.J. Groves, Analyst 99, 959 (1974).
2. T. Allen, "Particle Size Measurement", John Wiley and Sons, Inc., New York (1975).
3. H.C. Van de Hulst, "Light Scattering by Small Particles", John Wiley and Sons, New York (1957).
4. (i) R.M. Tabibiau, W. Heller and J.N. Epel, J. Colloid Sci., 11, 195 (1956).
(ii) M. Kerker, "The Scattering of Light and Other Electromagnetic Radiation", Academic Press, New York.
5. (i) H. Small, F.L. Saunders and J. Sole, Adv. Colloid Interface Sci., 6 (4), 237-266 (1976).
(ii) H. Small, J. Colloid Interface Sci., 48 (1), 147 (1974).
6. H. Coll, G.R. Fague and K.A. Robillard, "Exclusion Chromatography of Colloidal Dispersions", unpublished work, Eastman Kodak, Rochester, New York (1975).
7. V.F. Gaylor and H.L. James, Preprints-Pittsburg Conference on Analytical Chem., Cleveland, Ohio, March (1975).
8. K.F. Krebs and W. Wunderlich, Angew Makromolecules Chem., 20, 203 (1971).
9. C.M. Guttman and E.A. DiMarzio, Makromolecules, 3, 681 (1970).
10. R.F. Stoisits, G.W. Poehlein and J.W. Vanderhoff, J. Colloid Interface Sci., 57, 337 (1976).
11. A.J. McHugh, Hydrodynamic Chromatography for Latex Particle Size Distribution (in press).
12. E.A. DiMarzio and C.M. Guttman, J. Polym. Sci., Part B, 7, 267 (1969).
13. E.F. Cassassa, J. Phy. Chem., 75, 3929 (1971).
14. L.H. Tung, J. Appl. Polym. Sci., 10, 375 (1966).
15. K.H. Altgelt and L. Segal, "Gel Permeation Chromatography", Marcel Dekker Inc., New York (1971).
16. (i) T. Ishigee, S.I. Lee and A.E. Hamielec, J. Appl. Polym. Sci., 15, 1607 (1971).

- (ii) A.E. Hamielec, J. Appl. Polym. Sci., 14, 1519 (1970).
 - (iii) Nils Friis and A.E. Hamielec, Advances in Chromatography, Marcel-Dekker, Inc., New York, Vol. 13, p. 41.
17. T. Provder and E.M. Rosen, ACS Preprints, Houston (1970).
 18. D.D. Bly, W.W. Yau and H.J. Stoklasa, Analy. Chem., 48, 1256 (1976).
 19. A.R. Goodall, M.C. Wilkinson and J. Hearn, J. Colloid Interface Sci., 53, 327 (1975).

APPENDICES 9

9.1 Technique for the Measurement of Monomer Concentration in the Aqueous and in the Polymer Phase of an Emulsion Polymerization

In modeling an emulsion polymerization, it is normal practice to assume that the total amount of the monomer unreacted is in the polymer phase. This assumption could lead to significant amount of error if the monomer was fairly soluble in the aqueous phase and especially if the polymerization was being carried out under the monomer starved conditions.

An attempt was made to follow the concentration of vinyl acetate monomer in the aqueous phase of the emulsion polymerization by measuring the refractive index of the aqueous phase. Since the refractive index of pure water (1.3342) is very close to that of the saturated aqueous solution of vinyl acetate (1.3352), therefore this technique was rejected. Instead the analysis was done successfully with much better accuracy using analytical gas chromatograph. The latex was centrifuged at about 15000 rpm for 10-15 mins which separated the aqueous phase from the polymer phase. A few microliters of this aqueous layer were then injected into the chromatograph and the concentration of the vinyl acetate in aqueous phase was calculated. Since the total amount of unreacted monomer was known from the conversion-time history and hence the concentration of the monomer in the polymer phase was calculated. The concentrations of vinyl acetate in aqueous and in polymer phase are shown in Figure 15(a) for an emulsion polymerization along with their respective conversion-time history (in Figure 15(b)).

This technique can also be used to follow the concentration of byproducts of an emulsion or suspension polymerization, eg. Acetic acid in emulsion polymerization of vinyl acetate.

9.2 Method to Evaluate Frequency Distribution Function Variance and Total Number of Particles by Measuring the Turbidities at Two Different Wavelength Using a Light Scattering Detector

While doing the particle size analysis, one should measure the turbidities at two different wavelengths. The normalized chromatograms obtained at two wavelengths would superimpose if there is no chemical absorption. Table 20 compares the normalized heights of the chromatograms obtained for unknown sample. Table 21 shows the different diameter averages calculated from these two chromatograms. % Standard deviation among the values is within the experimental error.

While obtaining the corrected diameter averages, we need to know the variance. The calculated variance from the chromatogram may not be the real variance that should be used. Instead one can calculate the overall variance of the frequency distribution as follows:

At any point on the chromatogram the turbidities at the two wavelengths can be expressed as follows

$$\tau_{\lambda_1}(v) = \frac{1}{\sqrt{2\pi\sigma^2(v)}} \int_0^\infty K(\frac{D}{\lambda_1}, \frac{n}{n_m}) N(v) D^2(v) \exp(-(D_o - D(v))^2/2\sigma(v)^2) dv$$

$$\tau_{\lambda_2}(v) = \frac{1}{\sqrt{2\pi\sigma^2(v)}} \int_0^\infty K(\frac{D}{\lambda_2}, \frac{n}{n_m}) N(v) D^2(v) \exp(-(D_o - D(v))^2/2\sigma(v)^2) dv$$

where D_0 is the diameter equivalent to the peak position of the chromatogram. There are two unknowns $N(v)$ and $\sigma^2(v)$ and two equations, therefore one can evaluate the total number of particles or the frequency distribution function.

9.3 Computer Program

***THIS PROGRAM COMPUTES THE DIFFERENT DIAMETER AVERAGES FROM A GIVEN CHROMATOGRAM AND A LINEAR CALIBRATION CURVE AND IS BASED ON THE PROGRAM WRITTEN BY ISHIGE, LEE AND PAMELEC FOR CORRECTING THE INSTRUMENTAL SPREADING CORRECTION FOR MOLECULAR WEIGHT CALCULATIONS. SURENDRA SINGH, MAY 1977
GENERAL SHAPE FUNCTION WITH 3 PARAMETERS H, U AS INSTRUMENTAL SPREADING. WHEN A3 AND A4 ARE ZERO (GAUSSIAN SPREADING H IS ALLOWED TO VARY WITH SAMPLES OF DIFFERENT PARTICLE SIZES)

| | |
|------------|--|
| HEAD(I) | YOUR HEADING FOR COMPUTATION |
| CH(I) | QUADRATIC EXPRESSION FOR GAUSSIAN RESOLUTION FACTOR H $H=CH(1)+CH(2)*Y+CH(3)*Y^2$ |
| NCP | NO. OF DATA POINTS |
| V0, VF | RETENTION VOLUME OF THE FIRST AND LAST DATA POINTS |
| CINC | INTERVAL OF DATA POINTS (IN COUNTS) |
| HT(I) | HEIGHT OF YOUR CHROMATOGRAM |
| F0(I) | HEIGHT OF THE CHROMATOGRAM NORMALIZED |
| EV(I) | RETENTION VOLUME OF DATA POINTS |
| C1, C2 | LINEAR CALIBRATION CURVE PARAMETERS $\log_{10}(D) = (C1 - V)/C2$ |
| W(I) | INSTRUMENTAL SPREADING CORRECTED CHROMATOGRAM |
| G0(I) | GAUSSIAN SPREADING FUNCTION |
| GL(I) | GENERAL SHAPE FUNCTION LEFT SIDE FROM $V=Y$ |
| GR(I) | GENERAL SHAPE FUNCTION RIGHT SIDE FROM $V=Y$ |
| U2, U3, U4 | $2-NC, 3-RC \text{ AND } 4-TH MOMENT OF } G(V,Y)$ |
| A3 | $=U3/(U2^2)$ |
| A4 | $=U4/(U2^2) - 3$ |

DIMENSION HT(200), EV(200), F(200), F0(200), W(200), CH(7), HED(10), CELF(200), GELF(200), G0(50), GR(50), GL(50), D(50), ED(50),
2WC(50), FC(200), QSCAT(200)
DIMENSION THETC(100), ELTRMX(4, 100, 2)
COMMON A, E, CONST1, CONST2, SIGS, ALFA
COMMON SK(50)

HERMITE POLYNOMIALS
 $H3(X)=X^{**3}-3\cdot 0\cdot X$
 $H4(X)=X^{**4}-6\cdot 0\cdot (X^{**2})+3\cdot 0$

*** SPECIFY THE METHOD TO BE USED AND TOLERANCE
 METHCC=1
 METHCD=2
 TCL=0.01

*** OBTAIN THE VALUES OF A, B, CONST1 AND CONST2 BY FITTING THE SCAT. COEFF. DATA IN THE FOLLOWING FORM
 $1/SK(I) = CONST1 * EXP(A*V) + CONST2 * EXP(B*V)$

ALFA=0.
 A=1.307

```

B=0.08296
CONST1=0.7618E-07
CONST2=0.1211
SIGS=1.161
C *** READ IN DATA
READ (5,44) (HEAD(I),I=1,8)
READ (5,45) CH(1),CH(2),CH(3),A3,A4
READ (5,46) NOP,V0,VF,CINC
READ (5,47) (HT(I),I=1,NCP)
READ (5,48) C1,C2
DO 1 I=1,NOP
EV(I)=V0+CINC*FLOAT(I-1)
1 CONTINUE
CALL SIMPSON (EV,HT,CINC,NOP,AINTHT).
DO 2 I=1,NOP
FO(I)=HT(I)/AINTHT
2 CONTINUE
D2=2.303/C2
D1=EXP(C1*D2).

CC* COMPUTE THE SCATTERING COEFFICIENT
CCC
C
PI=4.0*ATAN(1.0)
JX=2
THETO(1)=0.
THETO(2)=0.0
RFI=0.0
RFR=1.195
RH=1.33
RP=RFR*RW
WL=2940.
WRITE (6,35) WL,RP,RW,RFR
ALM=WL/RW
DO 3 I=1,NOP
D(I)=D1*EXP(-D2*EV(I))
X=D(I)
ALP=PI*X/ALM
CALL OAHIE (ALF,RFR,RFI,THETO,JX,QEXT,SCATQ,CTBRS,ELTRMX)
SK(I)=SCATQ
WRITE (6,36) I,X,SK(I)
3 CONTINUE
WRITE (6,67) METHOD
WRITE (6,44) (HEAD(I),I=1,8)
WRITE (6,49) NOP,V0,VF,CINC
WRITE (6,72) C1,C2
IF (ABS(CH(2))+ABS(CH(3)).GT.0.0) GO TO 4
UNIFCRM=1.0
H=CH(1)
U2=1.0/(2.0*H)
U3=A3*(U2**1.5)
U4=(A4+3.0)*(U2**2)
WRITE (6,50) H,U2,U3,A3,U4,A4
IF (A3.EQ.0.0.AND.A4.EQ.0.0) WRITE (6,68)
GO TO 5
4 UNIFCRM=-1.0

```

```

      WRITE (6,51) CH(1),CH(2),CH(3)
E     CCNTINUE
C. *** IF G(V,Y) IS UNIFORM, APPLY ANALYTICAL CORRECTION
      IF (UNIFORM.LT.0.0) GO TO 11
      WRITE (6,52)
      WRITE (6,53) (EV(I),D(I),HT(I),FD(I),I=1,NOP)

CCCCC
      CALCULATE THE DIAMETER AVERAGES

CCCCC
      L=1
      CALL AVEDIAM (EV,FD,CINC,NOP,C1,C2,DNOO,DSOO,DSSOO,DWOO,DVOO,DTAUC
      10, CNTRUE, DSTRUE, DSSTRUE, DWTRUE, DVTRUE, DTAUTRU, FD, WD, L)
      WRITE (6,37) DNOO,DSOO,DSSOO,DWOO,DVOO,DTAUOO
      L=2
      CALL AVEDIAM (EV,FD,CINC,NOP,C1,C2,DNOO,DSOO,DSSOO,DWOO,DVOO,DTAUC
      10, DNTRUE, CSTRUE, DSSTRUE, CWTRUE, DVTRUE, DTAUTRU, FD, WD, L)
      WRITE (6,54) DNOO,CSOO,DSSOO,DWOC,DVOO,DTAUOO,CNTRUE,DSTRUE,DSSTRU
      1E, DWTRUE,CVTRUE,DTAUTRU
      WRITE (6,38)
      DO 6 I=1,NOP
      WRITE (6,41) D(I),FD(I),WD(I)
      CONTINUE
      DO 7 I=1,NOP
      CALL PLOTPT (D(I),FD(I),9)
      CALL PLOTFT (D(I),WD(I),4)
      7    CCNTINUE
      CALL OUTPLT
      WRITE (6,39)
      WRITE (6,43)
      NOP=NOP-1
      DO 8 I=2,NOP
      D(I)= ALOG(D(I))
      FD(I)= ALOG(ABS(FD(I)))
      WD(I)= ALOG(ABS(WD(I)))
      WRITE (6,42) D(I),FD(I),WD(I)
      CALL PLOTPT (D(I),FD(I),9)
      CALL PLOTFT (D(I),WD(I),4)
      8    CONTINUE
      CALL OUTPLT
      WRITE (6,40)
      NOP=NOP+1
C     CALL SMOOTH (FD,NOP)
C     WRITE (6,55)
C     CALL GRAPH1 (EV,FD,0.5,NOP)

CCCCC
      *** STORE THE SHAPE OF G(V,Y) WHEN IT IS UNIFORM
      WRITE (6,69) H,U3,U4
      PAI=3.1415926
      JOEL=NOP
      CONS1=SQRT(H/PAI)
      CONS2=SQRT(2.0*H)
      DO 9 I=1,JOEL

```

```

FIM1=I-1
DELV=FIM1*CINC
DELV2=DELV**2
X=CCNS2*DELV
G0(I)=CONS1*EXP(-H*DELV2)
GR(I)=(1.0+(A3/6.0)*H3(X)+(A4/24.0)*H4(X))*G0(I)
GL(I)=(1.0+(A3/6.0)*H3(-X)+(A4/24.0)*H4(-X))*G0(I)
WRITE(6,70) DELV,G0(I),GL(I),GR(I)
IF (GR(I).LT.0.0) GR(I)=0.0
IF (GL(I).LT.0.0) GL(I)=0.0
9 CONTINUE
WRITE(6,71)
CALL SIMPSON(EV,GR,CINC,JOEL,AINTGR)
CALL SIMPSON(EV,GL,CINC,JOEL,AINTGL)
AREA=AINTGR+AINTGL
DO 10 I#1,JOEL
GR(I)=GR(I)/AREA
GL(I)=GL(I)/AREA
10 CONTINUE
JOELP1=JOEL+1
GO(JOELP1)=GR(JOELP1)=GL(JOELP1)=0.0
GO TO 12
11 WRITE(6,56)
12 CONTINUE
C
C
13 WRITE(6,57) METHOD
14 WRITE(6,58)
IF (METHOD.EQ.2) GO TO 24
C *** YOU ENTERED METHOD0-1, ADD 50 MORE DATA POINTS AT BOTH ENDS.
C
15 NOP50=NOP+50
16 NOP51=NOP+51
17 NOP100=NOP+100
DO 13 I=1,NOP
HT(I)=FO(I)
13 CONTINUE
DO 14 I=1,50
FO(I)=0.0
14 CONTINUE
DO 15 I=51,NOP50
FO(I)=HT(I-50)
15 CONTINUE
DO 16 I=NOP51,NOP100
FO(I)=0.0
16 CONTINUE
DO 17 I=1,NOP100
EV(I)=VO+CINC*FLOAT(I-51)
17 CONTINUE
C *** DEFINE INITIAL DELF(I) AND H(I)
K=0
DO 18 I=1,NOP100
DELF(I)=H(I)=FO(I)
18 CONTINUE
C

```

```

C *** COMPUTE NEW DELF(I), CORRECT W(I) AND CHECK AREA DIFFERENCE
19 K=K+1
    IF (UNIFORM.LT.0.0) GO TO 20
    CALL GROSEN (GR,GL,EV,DELF,CINC,NDF100,JOEL,GDEL)
    GO TO 21
20  CALL GNONUNI (EV,DELF,CINC,NCP100,CH,GDEL)
    CONTINUE
    DELS=0.0
    DO 22 I=1,NDF100
        DELF(I)=DELF(I)-GDEL(I)
        DELS=ABS(DELF(I))*CINC+DELS
        W(I)=W(I)+DELF(I)
22  CONTINUE
    WRITE (6,59) K,DELS
    IF (DELS.LT.TOL) GO TO 23
    GO TO 19
23  CONTINUE
    IF (UNIFORM.GT.0.0) CALL GROSEN (GR,GL,EV,W,CINC,NDF100,JOEL,F)
    IF (UNIFORM.LT.0.0) CALL GNONUNI (EV,W,CINC,NDF100,CH,F)
    GO TO 34
C
C *** YOU ENTERED METHOD-2
24  CONTINUE
C
C *** ASSUME W(Y)=F0(V) AND COMPUTE G(W)
25  K=1
    DO 25 I=1,NDF
        W(I)=F0(I)
    CONTINUE
    DELS=100.0
C
C *** ITERATION FOLLOWS
26  CONTINUE
    IF (UNIFORM.LT.0.0) GO TO 27
    CALL GROSEN (GF,GL,EV,W,CINC,NDF,JOEL,F)
    GO TO 28
27  CALL GNONUNI (EV,W,CINC,NDF,CH,F)
    CONTINUE
    SUM=0.0
    DO 29 I=1,NDF
        DIFF=F(I)-F0(I)
        SUM=ABS(DIFF)*CINC+SUM
29  CONTINUE
    WRITE (6,59) K,SUM
    IF (DELS.LT.SUM) GO TO 33
    DELS=SUM
    IF (DELS.LT.TOL) GO TO 34
    K=K+1
    DO 31 I=1,NDF
        IF (F0(I).GT.0.0) GO TO 30
        HT(I)=0.0
        GO TO 31
30  HT(I)=(F0(I)/F(I))*W(I)
    CONTINUE
    CALL SIMPSON (EV,HT,CINC,NDF,AINTHT)
    DO 32 I=1,NDF

```

```

32      W(I)=HT(I)/AINTHT
CONTINUE
GO TO 26
33      CONTINUE
C
C *** PRINT OUT THE RESULTS
C
34      CONTINUE
WRITE (6,60) K
WRITE (6,61)
IF (METHOD.EQ.1) NCP=NDP100
WRITE (6,62) (EV(I),W(I),F(I),FO(I),I=1,NOP)
CALL AVEDIAM (EV,W,CINC,NDP,C1,C2,DN00,DS00,DSS00,DW00,DV00,DTAU00
1, DNTRUE,DSTRUE,DSSTRUE,DHTRUE,DVTRUE,DTAUTRU,FD,W0,L)
WRITE (6,64) DKO0,CS00,DSS00,DW00,CV00,DTAU00
IF (DELS.LT.TOL) WRITE (6,63)
WRITE (6,65)
CALL GRAPH1 (EV,W,0.5,NDP)
WRITE (6,66)
CALL GRAPH1 (EV,F,0.5,NDP)
STOP
C
C
C
35      FORMAT (1H1,30X,*WAVE-LENGTH = *,F10.2,10X,*REFRACTIVE INDEX OF P
10LYMER = *,F10.5,11X,*REFRACTIVE INDEX OF SOLVENT = *,F10.5,10X,
2*RATIO OF REFRACTIVE INCICES = *,F10.5,11X)
36      FORMAT (19X,I8,10X,F6.0,10X,E2[.5])
37      FORMAT (1H1,12X,*UNCORRECTED DIAM. AVERAGES USING THE SCATT.
1COEFFICIENTS//20X,*DNGO = *,F10.0//20X,*DS00 = *,F10.0//20X
2,*DSS00 = *,F10.0//20X,*DW00 = *,F10.0//20X,*DV00 = *,F10.0//
320X,*DTAU00 = *,F10.0)
38      FORMAT (1H1,15X,*D(I)*,6X,*FO(I)*,11X,*WD(I)*//)
39      FORMAT (//,* F(D) AND W(D) .VS. PARTICLE DIAMETER*)
40      FORMAT (//,* LOG F(D) AND LOG W(D) .VS. LOG D(I)*)
41      FORMAT (1CX,F10.0,2E15.4)
42      FORMAT (13X,F10.2,6X,E15.4,2X,E15.4)
43      FORMAT (1H1,15X,* LOGO(I)*,10X,* LOG F(C)*8X,*LOG W(D)*//)
44      FORMAT (8A10)
45      FORMAT (5F10.5)
46      FORMAT (I10,7F10.2)
47      FORMAT (16F5.0)
48      FORMAT (2F10.4)
49      FORMAT (1H0,10X,*NO. OF GIVEN DATA POINT * * * * * ,I3/11X,*E.V. OF
1 1-ST POINT * * * * * ,F6.2/11X,*E.V. OF LAST POINT * * * * * *
2,*F6.2/11X,*DATA POINT INTERVAL BY COUNT * * * * * ,F6.2/)
50      FORMAT (11X,*GENERAL SHAPE FUNCTION G(H,L3,U4)*16X,*H = *,F6.4,2X
1,*{ U2 = *,F6.3}*15X,*U3 = *,F6.3,2X,*{ A3 = *,F6.3,* }*15X,*U4 = *,F6.6,2X,*{ A4 = *,F6.3,* }*)
51      FORMAT (11X,*NCN-UNIFORM GAUSSIAN SPREADING WITH VARIABLE H*/15X,*H = CH(1) + CH(2)*Y + CH(3)*Y*Y*/20X,*CH(1) = *,F6.3/20X,*CH(2) = *F6.3/20X,*CH(3) = *,F6.3//)
52      FORMAT (25X,*OBSERVED LEC CHROMATOGRAM//20X,*EV(I)*,10X,*D(I)*,12
1X,*HT(I)*,9X,*FO(I)*//)
53      FORMAT (19X,F6.2,10X,F6.0,10X,F5.0,7X,F8.4)
54      FORMAT (//,*14X,*UNCORRECTED DIAM. AVERAGES USING THE EXPONENTIAL
1 FIT//20X,*DN00 = *,F10.0//20X,*DS00 = *,F10.0//20X,*DSS00

```

```

2 = *,F10.0//20X,*DWOO = *,F10.0//20X,*DVOO = *,F10.0//20X,*DT
3AU00 = *,F10.0///14X,*CCRRECTED DIAM. AVERAGES USING THE EXPONENT
4IAL FIT*///20X,*DNTRUE = *,F10.0//20X,*DSTRUE = *,F10.0//20X,*D
5SSTPUE = *,F10.0//20X,*DHTRUE = *,F10.0//20X,*DVTRUE = *,F10.0//2
620X,*DTAUTRUE= * F10.0)
5 FORMAT (1H1,30X,*REPRODUCTION OF THE OBSERVED CHROMATOGRAM F0*)/
56 FORMAT (15X,*ANALYTICAL CORRECTION NOT APPLICABLE*)
57 FORMAT (1H0,20X,*SEARCH FOR W(Y) BY METHOD-*,I1,* NOW FOLLOWS*)
58 FORMAT (1H0,18X,*K*,10X,*DELS*)
59 FORMAT (10X,I10,5X,F10.4)
60 FORMAT (1H1,10X,*W(Y) OBTAINED AT*,I3,*-TH ITERATION*)
61 FORMAT (15X,*EV(I)*,10X,*W(I)*,9X,*F(I)=G(W(I))*,3X,*OBSERVED F0(I
1)*)
62 FORMAT (10X,F10.2,3F15.4)
63 FORMAT (1H0,10X,*... TUNG'S EQUATION SATISFIED WITHIN TOL.*)
64 FORMAT (1H1,14X,*CORRECTED DIAMETER AVERAGES *///20X,*DNCORR =
1*,F10.0//20X,*DSCORR = *,F10.0//20X,*DSSCORR = *,F10.0//20X,*DWCO
2RR = *,F10.0//20X,*DVCORR = *,F10.0//20X,*DTAUCORR= *,F10.0)
65 FORMAT (1H1,10X,*SHAPE OF W OBTAINED*)
66 FORMAT (1H1,10X,*SHAPE OF F WITH THE ABOVE W*)
67 FORMAT (1H1,19X,50(1H*)/20X,1H*,48X,1H*/20X,1H*,5X,*PROGRAM---LEC
1SPREADING CORRECTION*,9X,1H*/20X,1H*,15X,*METHOD -*,I2,23X,1H*/20X
2,1H*,48X,1H*/20X,50(1H*)//)
68 FORMAT (20X,*THIS G IS AN UNIFORM GAUSSIAN*)
69 FORMAT (1H0,20X,*SHAPE OF YOUR GENERAL SPREADING FUNCTION G(V,Y)*/
130X,*H = *,F7.4/30X,*U3 = *,F6.2/30X,*U4 = *,E8.1//17X,*V-Y*,5X,*G
20(V-Y)=G0(-(V-Y))* ,5X,*G(-(V-Y))* ,5X,*G(V-Y)*/)
70 FORMAT (10X,F10.2,3F15.5)
71 FORMAT (25X,*NEGATIVE PORTION(IF ANY) IN THE ABOVE G(V,Y)*/25X,*IS
1 SET ZERO AND THE SHAPE NORMALIZED FOR USE*)
72 FORMAT (11X,*LINEAR CALIBRATION CURVE LOG10(D) = (*,F8.4,* - V )/*
1,F6.4*)
END

```

SUBROUTINE AVFCIAM (X,Y,DELX,N,C1,C2,CMOC,OSOO,DSSCO,CHOC,CVOC,DTA
 1UCC,ENTRUE,CSTFUE,DSSFCUE,CHOCUE,DTAUTE,{,FQ,W,L)
 DIMENSION X(200), Y(200), BAKA1(200), BAKA2(200), BAKA3(200), BAKA4(200)
 14(200), BAKA5(200), BAKA6(200), BAKA7(200), BAKA8(200), BAKA9(200), BAKA10(200)
 2, BAKA11(200), BAKA12(200), BAKA13(200), BAKA14(200), BAKA15(200),
 3 BAKA16(200), BAKA17(200), BAKA18(200), BAKA19(200), BAKA20(200),
 4 BAKA21(200), BAKA22(200), BAKA23(200), BAKA24(200), F
 5,(200), WC(200)
 COMMON A,B,CONST1,CONST2,SIGS,ALFA
 COMMON SK(50)

** THIS SUBROUTINE COMPUTES THE DIFFERENT DIAMETER AVERAGES
 FROM A GIVEN CHROMATOGRAM AND A LINEAR CALIBRATION CURVE
 OF THE FORM $\log_{10}(C) = (C1 - V)/C2$

```

D2=2.303/C2
D1=EXP(C1*D2)
HSIGS=SIGS/2.
RATIO=CONST2/CONST1
AP1=(A+D2)
BP1=(B+D2)
AM1=(A-D2)
BM1=(B-D2)
AP2=(A+2.*D2)
BP2=(B+2.*D2)
AM2=(A-2.*D2)
BM2=(B-2.*D2)
AM3=(A-3.*D2)
BM3=(B-3.*D2)
AM4=(A-4.*D2)
BM4=(B-4.*D2)
DO 2 I=1,N
IF (L.EQ.1) GO TO 1
SK(I)=1./(C0+ST1-X*(A-X(I))+CONST2*EXP(B*X(I)))
BAKA1(I)=(Y(I)*EXP(C2*X(I)))/(SK(I))
BAKA2(I)=(Y(I)*EXP(2.*C2*X(I)))/(SK(I))
BAKA3(I)=(Y(I)*EXP(-4.*D2*X(I)))/(SK(I))
BAKA4(I)=(Y(I)*EXP(-3.*D2*X(I)))/(SK(I))
BAKA5(I)=(Y(I)*EXP(+3.*D2*X(I)))/(SK(I))
BAKA6(I)=(Y(I)*EXP(0.+D2*X(I)))/(SK(I))
BAKA7(I)=(Y(I)*EXP(-2.+D2*X(I)))/(SK(I))
BAKA8(I)=(Y(I)*EXP(-5.+D2*X(I)))/(SK(I))
BAKA9(I)=(Y(I)*EXP(4*M4*X(I)))
BAKA10(I)=(Y(I)*EXP(9*M4*X(I)))
BAKA11(I)=(Y(I)*EXP(4*M3*X(I)))
BAKA12(I)=(Y(I)*EXP(8*M3*X(I)))
BAKA13(I)=(Y(I)*EXP(8*M1*X(I)))
BAKA14(I)=(Y(I)*EXP(2*M1*X(I)))
BAKA15(I)=(Y(I)*EXP(4*M1*X(I)))
BAKA16(I)=(Y(I)*EXP(4*X(I)))
BAKA17(I)=(Y(I)*EXP(B*X(I)))
BAKA18(I)=(Y(I)*EXP(B*X(I)))
BAKA19(I)=(Y(I)*EXP(4*P2*X(I)))
BAKA20(I)=(Y(I)*EXP(8*P2*X(I)))
BAKA21(I)=(Y(I)*EXP(4*M2*X(I)))
BAKA22(I)=(Y(I)*EXP(8*M2*X(I)))
BAKA23(I)=(Y(I)*EXP(4*P1*X(I)))

```

```

BAKA24 (I)=(Y(I)*FXF(RF1*X(I)))
2
CONTINUE
CALL SIMPSON (X,BAKA1,DELX,N,AINT1)
CALL SIMPSON (X,BAKA2,DELX,N,AINT2)
CALL SIMPSON (X,BAKA3,DELX,N,AINT3)
CALL SIMPSON (X,BAKA4,DELX,N,AINT4)
CALL SIMPSON (X,BAKA5,DELX,N,AINT5)
CALL SIMPSON (X,BAKA6,DELX,N,AINT6)
CALL SIMPSON (X,BAKA7,DELX,N,AINT7)
CALL SIMPSON (X,BAKA8,DELX,N,AINT8)
CALL SIMPSON (X,BAKA9,DELX,N,AINT9)
CALL SIMPSON (X,BAKA10,DELX,N,AINT10)
CALL SIMPSON (X,BAKA11,DELX,N,AINT11)
CALL SIMPSON (X,BAKA12,DELX,N,AINT12)
CALL SIMPSON (X,BAKA13,DELX,N,AINT13)
CALL SIMPSON (X,BAKA14,DELX,N,AINT14)
CALL SIMPSON (X,BAKA15,DELX,N,AINT15)
CALL SIMPSON (X,BAKA16,DELX,N,AINT16)
CALL SIMPSON (X,BAKA17,DELX,N,AINT17)
CALL SIMPSON (X,BAKA18,DELX,N,AINT18)
CALL SIMPSON (X,BAKA19,DELX,N,AINT19)
CALL SIMPSON (X,BAKA20,DELX,N,AINT20)
CALL SIMPSON (X,BAKA21,DELX,N,AINT21)
CALL SIMPSON (X,BAKA22,DELX,N,AINT22)
CALL SIMPSON (X,BAKA23,DELX,N,AINT23)
CALL SIMPSON (X,BAKA24,DELX,N,AINT24)

```

```

C
4C
JHCC=D1*(AINT1/ATNT2)
JSOC=D1*(AINT3/ATNT2)**(1./2.)
JSSCC=D1*(AINT4/ATNT3)
JWCC=D1*(AINT9/ATNT4)
JVCC=D1*(AINT14/ATNT2)**(1./3.)
JTAUCC=D1*(AINT3/AINT4)**(1./3.)
JEGCC=D1*(AINT3/AINT5)

```

```

C
C
AAM4=(AINT11/((EXP((AM4**2.)*HSIGS))*(1.-ALFA
1.(AM4**3.))))
3BM4=(AINT12/((EXP((BM4**2.)*HSIGS))*(1.-ALFA
1.(BM4**3.)))*RATIO
AAM3=(AINT13/((EXP((AM3**2.)*HSIGS))*(1.-ALFA
1.(AM3**3.))))
3BM3=(AINT14/((EXP((BM3**2.)*HSIGS))*(1.-ALFA
1.(BM3**3.)))*RATIO
AAM1=(AINT15/((EXP((AM1**2.)*HSIGS))*(1.-ALFA
1.(AM1**3.))))
3BM1=(AINT16/((EXP((BM1**2.)*HSIGS))*(1.-ALFA
1.(BM1**3.)))*RATIO
AAA= (AINT17/((EXP((A**2.)*HSIGS))*(1.-ALFA
1.(A**3.))))
3BB= (AINT18/((EXP((B**2.)*HSIGS))*(1.-ALFA
1.(B**3.)))*RATIO
AAP2=(AINT19/((EXP((AP2**2.)*HSIGS))*(1.-ALFA
1.(AP2**3.))))
3BP2=(AINT20/((EXP((BP2**2.)*HSIGS))*(1.-ALFA
1.(BP2**3.)))*RATIO
AAM2=(AINT21/((EXP((AM2**2.)*HSIGS))*(1.-ALFA
1.(AM2**3.))))

```

```

99M2= (AINT22/ (( EXP(( EM2**2.) * HSIGS)) * ( 1.- ALFA *
1 (B2**3.)))) * RATIO
1 AAP1= (AINT23/ (( EXP(( AP1**2.) * HSIGS)) * ( 1.- ALFA *
1 (AF1**3.))))
1 BEP1= (AINT24/ (( EXP(( BP1**2.) * HSIGS)) * ( 1.- ALFA *
1 (BF1**3.)))) * RATIO

DNTRUE=D1* ((AAF1+BEP1)/(AAP2+BEP2))
DSTRUE=D1* ((AAA1+BPM1)/(AAP2+BPM2))** (1./2.)
DSSTRUE=D1* ((AAW1+BPM1)/(AAA1+BPM1))
DWTRUE=D1* ((AAW2+BPM2)/(AAW1+BPM1))
DVTRUE=D1* ((AAW1+BPM1)/(AAP2+BEP2))** (1./3.)
DTAUTRU=D1* ((AAW4+BPM4)/(AAW1+BPM1))** (1./3.)
DE5TRUE=D1* ((AAW4+BEW4)/(AAW3+BPM3))

DC 3 I=1,N
FD(I)=(BAKA6(I)/AIN2)*(1./(D1*D2))
CONTINUE
DO 4 I=1,N
BAKA7(I)=(FD(I)*EXP(-3.*C2*X(I)))
CONTINUE
CALL SIMPSON (X,RAKA7,CEIX,N,AJ'(T7)
DC 5 I=1,N
WD(I)=(FD(I)*EXP(-3.*C2*X(I))/AIN7)
CONTINUE
RETURN
END

```

```

SUBROUTINE GRAPH1 (X,Y,YMAX,N)
REAL X(200),Y(200),LINE(101)

C *** THIS SUBPROGRAM PLOTS Y AGAINST X
C
DATA BLANK,DOT,PLUS,MINUS,STAR,BATSU/1H ,1H.,1H+,1H-,1H*,1HX/
WRITE (6,10) YMAX
WRITE (6,11)
DO 1 I=1,101
LINE(I)=DOT
1 CONTINUE
DO 2 I=1,101,5
LINE(I)=PLUS
2 CONTINUE
LINE(1)=BATSU
WRITE (6,8) LINE
DO 3 I=1,101
LINE(I)=BLANK
3 CONTINUE
DO 5 I=1,N
SIGN=1.0
IF (Y(I).LT.0.0) SIGN=-1.0
LINE(1)=LINE(101)=PLUS
PLACE=ABS(Y(I)*100.0/YMAX)+1.0
IPLACE=IFIX(PLACE)
IF (IPLACE.GT.101) IPLACE=101
LINE(IPLACE)=STAR
IF (SIGN.LT.0.0) LINE(IPLACE)=DOT
IF (((I-1)/5)*5.EQ.(I-1)) GO TO 4
WRITE (6,8) LINE
GO TO 5
4 LINE(1)=LINE(101)=BATSU
WRITE (6,9) X(I),LINE
5 LINE(IPLACE)=BLANK
DO 6 I=1,101
LINE(I)=DOT
6 CONTINUE
DO 7 I=1,101,5
LINE(I)=PLUS
7 CONTINUE
WRITE (6,8) LINE
RETURN

C
8 FORMAT (20X,101A1)
FORMAT (10X,F10.2,101A1)
9 FORMAT (55X,*FULL SCALE = *,F7.3)
10 FORMAT (1F0,17X,* 0.0*,6X,* 0.1*,6X,* 0.2*,7X,* 0.3*,7X,* 0.4*,7X,* 0
11 1.5*,7X,* 0.6*,7X,* 0.7*,7X,* 0.8*,7X,* 0.9*,7X,* 1.0*)
END

```

```

SUBROUTINE GROSEN (GR,GL,X,Y,DELX,N,JDEL,GY)
DIMENSION X(200), Y(200), GY(200), GR(200), GL(200)

C *** THIS PROGRAM CARRIES OUT G-OPERATION FOR GENERAL SHAPE FUNCTION WI
THREE PARAMETERS H, U3 AND U4. THESE PARAMETER MUST BE CONSTANT.

C
DO 4 I=1,N
SUMXJ=0.0
JBEGIN=I-JDEL
JEND=I+JDEL
IF (JBEGIN.LT.1) JBEGIN=1
IF (JEND.GT.N) JEND=N
DO 3 J=JBEGIN, JEND
IF (Y(J).EQ.0.0) GO TO 3
FIMJ=I-J
IJ=AES(FIMJ)+1.0
IF (I.LT.J) GO TO 1
GYXJ=Y(J)*GR(IJ)
GC TO 2
1 GYXJ=Y(J)*GL(IJ)
SUMXJ=SUMXJ+GYXJ*DELX
CONTINUE
2 GY(I)=SUMXJ
CONTINUE
RETURN
END

```

SUBROUTINE SMOOTH (F,NPTS)

```

***** DATA SMOOTHING SUBROUTINE. METHOD= 7 POINTS CUBIC *****

DIMENSION F(NPTS)
DIMENSION Y(7,4), G(300)
DATA Y/39.0E00,8.0E00,-4.0E00,-4.0E00,1.0E00,4.0E00,-2.0E00,8.0E00
1,19.0E00,16.0E00,6.0E00,-4.0E00,-7.0E00,4.0E00,-4.0E00,16.0E00,19.
2)E00,12.0E00,2.0E00,-4.0E00,1.0E00,-4.0E00,6.0E00,12.0E00,14.0E00,
312.0E00,6.0E00,-4.0E00/
NPTS1=NPTS+1
NPTSZ=NPTS-6
DO 2 I=1,3
SUM=0.0E00
SUMEND=0.0E00
DO 1 J=1,7
SUM=SUM+Y(J,I)*F(J)
SUMEND=SUMEND+Y(J,I)*F(NPTS1-J)
CONTINUE
1 G(I)=SUM/YS
G(NPTS1-I)=SUMEND/YS
2 CONTINUE
DO 4 I=1,NPTSZ
K=I+3
SUM=0.0E00
DO 3 J=1,7
SUM=SUM+Y(J,4)*F(I+J-1)
CONTINUE
3 G(K)=SUM/YS
4 CONTINUE
DO 5 I=1,NPTS
F(I)=G(I)
IF (F(I).LT.0.0E00) F(I)=0.0E00
CONTINUE
5 RETURN
END

```

```

SUBROUTINE SIMPSON (X,Y,DELX,N,AINTY)
DIMENSION X(200), Y(200)
C *** THIS SUBPROGRAM EVALUATES THE INTEGRAL Y(X)DX IN GIVEN RANGE OF X
C BY SIMPSONS RULE.
C
NBAKA=1
IF ((N/2)*2,NE.N) GO TO 1
NBAKA=2
N=N+1
Y(N)=0.0
X(N)=X(N-1)+DELX
CONTINUE
1 NM1=N-1
NM2=N-2
SUMCCD=0.0
SUMEVEN=0.0
DO 2 I=2,NM1,2
SUMEVEN=SUMEVEN+Y(I)
CONTINUE
2 DO 3 I=3,NM2,2
SUMODD=SUMODD+Y(I)
CONTINUE
3 SUM=Y(1)+4.0*SUMEVEN+2.0*SUMODD+Y(N)
AINTY=DELX*SUM/3.0
IF (NBAKA.EQ.2) N=N-1
RETURN
END

```

```

SUBROUTINE GNQNUMI (X,Y,DELX,N,CRULEX,GY)
DIMENSION X(200), Y(200), CRULEX(3), GY(200)
C *** THIS SUBPROGRAM CARRIES OUT G-OPERATION FOR NON-UNIFORM GAUSSIAN
C SPREADING. RESOLUTION FACTOR H IS GIVEN BY A QUADRATIC EQUATION OF
C INPUT SPECIES, H=CRULEX(1)+CRULEX(2)*X+CRULEX(3)*X**2
C
PAI=3.1415926
DO 2 I=1,N
SUMXJ=0.0
DO 1 J=1,N
IF (Y(J).EQ.0.0) GO TO 1
HXJ=CRULEX(1)+CRULEX(2)*X(J)+CRULEX(3)*X(J)*X(J)
GYXJ=Y(J)*SQRT(HXJ/PAI)*EXP(-HXJ*(X(I)-X(J))**2)
SUMXJ=SUMXJ+GYXJ*DELX
1 CONTINUE
GY(I)=SUMXJ
2 CONTINUE
RETURN
END

```

SUBROUTINE DMBIE (X,RFF,RFI,THETO,JX,QEXT,OSCAT,CTBROS,ELTRMX)
 SUBROUTINE FOR COMPUTING THE PARAMETERS OF THE ELECTROMAGNETIC
 RADIATION SCATTERED BY A SPHERE. THIS SUBROUTINE CARRIES OUT ALL
 X- SIZE PARAMETER OF THE SPHERE, (2 * PI * RADIUS OF THE SPHERE)/
 WAVELENGTH OF THE INCIDENT RADIATION).
 RF- REFRACTIVE INDEX OF THE MATERIAL OF THE SPHERE.COMPLEX
 QUANTITY..FORM-(PFR-I*RFI)
 THIS SUBROUTINE WILL NOT GIVE RELIABLE RESULTS IF RFI * X IS
 GREATER THAN 80.0. IF SO, A MESSAGE IS PRINTED AND THE
 COMPUTATIONS ARE CONTINUED, SUGGEST USE DBMIE..
 THETO(J)- ANGLE IN DEGREES BETWEEN THE DIRECTIONS OF THE INCIDENT
 AND THE SCATTERED RADIATION. THETO(J) IS LESS OR = 90.0
 IF THETO(J) SHOULD HAPPEN TO BE GREATER THAN 90.0, ENTER WITH
 SUPPLEMENTARY VALUE. SEE COMMENTS BELOW ON ELTRMX..
 JX-TOTAL NUMBER OF THETO FOR WHICH THE COMPUTATIONS ARE
 REQUIRED. JX SHOULD NOT EXCEED 100 UNLESS THE DIMENSIONS
 STATEMENTS ARE APPROPRIATELY MODIFIED.
 MAIN PROGRAM SHOULD ALSO HAVE REAL *8 THETO(100), ELTRMX(4,100,2)
 THE DEFINITIONS FOR THE FOLLOWING SYMBOLS CAN BE FOUND IN *LIGHT
 SCATTERING BY SMALL PARTICLES, H.C. VAN DE HULST, JOHN WILEY AND
 SONS, INC., NEW YORK, 1957*.
 QEXT-EFFICIENCY FACTOR FOR EXTINCTION, VAN DE HULST, P.14, 127.
 OSCAT-EFFICIENCY FACTOR FOR SCATTERING, VAN DE HULST, P.14, 127.
 CTBROS-AVERAGE (COSINE THETA)* OSCAT, VAN DE HULST, P.128.
 ELTRMX(I,J,K)-ELEMENTS OF THE TRANSFORMATION MATRIX F, VAN DE
 HULST, P. 34, 45, 125. I=1-ELEMENT M SUB 2..I=2-ELEMENT M SUB 1..
 I=3-ELEMENT S SUB 21..I=4-ELEMENT O SUB 21..
 ELTRMX(I,J,1) REPRESENTS THE ITH ELEMENT OF THE MATRIX FOR
 THE ANGLE THETO(J)..ELTRMX(I,J,2) REPRESENTS THE ITH ELEMENT
 OF THE MATRIX FOR THE ANGLE 180.0-THETO(J)..
 DIMENSION T(5), TA(4), TB(2), TC(2), TD(2), TE(2)
 DIMENSION ELTRMX(4,100,2), PI(3,100), TAU(3,100), CSTHT(100)
 DIMENSION S12TH(100), THETO(100)
 COMPLEX RF, RRF, RRFX, WM1, FNA, FNE, TC1, TC2, WFN(2), ACAP(2)
 COMPLEX FNAP, FNBP
 EQUIVALENCE (WFN(1), TA(1)), (FNA, TB(1)), (FNB, TC(1))
 EQUIVALENCE (FNAP, TD(1)), (FNBP, TE(1))
 ST=4.0*ATAN(1.0)
 TA(1)-REAL PART OF WFN(1).. TA(2)-IMAGINARY PART OF WFN(1)..
 TA(3)-REAL PART OF WFN(2).. TA(4)- IMAGINARY PART OF WFN(2).
 TB(1)-REAL PART OF FNA..TB(2)- IMAGINARY PART OF FNA..
 TC(1)-REAL PART OF FNB..TC(2)- IMAGINARY PART OF FNB..
 TD(1)-REAL PART OF FNAP..TD(2)- IMAGINARY PART OF FNAP.
 TE(1)-REAL PART OF FNBP..TE(2)- IMAGINARY PART OF FNBP.
 FNAP + FNBP ARE THE PRECEDING VALUES OF FNA + FNB RESPECTIVELY.
 IF (JX.LE.100) GO TO 1
 WRITE (6,20)
 WRITE (6,19)
 CALL EXIT
 1 RF=CNPLX(RFR,-RFI)
 QRF=1.00/RF
 RX=1.00/X
 RRFX=RFR*RX
 DO 5 J=1,JX
 IF (THETO(J).LT.0.00) THETO(J)=ABS(THETO(J))
 IF (THETO(J).GT.0.00) GO TO 2
 CSTHT(J)=1.00

```

SI2THT(J)=0.00
GO TO 5
2 IF (THETO(J).GE.90.0) GO TO 3
T(1)=(ST*THETO(J))/180.0
CSTHT(J)=COS(T(1))
SI2THT(J)=1.00-CSTHT(J)**2
GO TO 5
3 IF (THETO(J).GT.90.0) GO TO 4
CSTHT(J)=0.00
SI2THT(J)=1.00
GO TO 5
4 WRITE (6,18) THETO(J)
WRITE (6,19)
CALL EXIT
5 CONTINUE
DO 6 J=1,JX
PI(1,J)=0.00
PI(2,J)=1.00
TAU(1,J)=0.00
TAU(2,J)=CSTHT(J)
6 CONTINUE
T(1)=COS(X)
T(2)=SIN(X)
WM1=CMPLX(T(1),-T(2))
WFn(1)=CMPLX(T(2),T(1))
WFN(2)=RX*WFN(1)-WM1
T(1)=RFX*X
IF (T(1).GT.80.0) GO TO 7
T(3)=0.5*EXP(T(1))
T(4)=0.25/T(3)
T(1)=T(3)+T(4)
T(2)=T(3)-T(4)
T(3)=T(2)**2
T(2)=T(1)*T(2)
T(1)=T(3)
T(3)=RFX*X
T(4)=SIN(T(3))
T(3)=COS(T(3))
T(1)=T(1)+T(4)**2
T(3)=T(3)*T(4)
ACAP(1)=CMPLX(T(3),T(2))/T(1)
GO TO 8
7 ACAP(1)=CMPLX(0.000,1.000)
WRITE (6,21) T(1)
WRITE (6,19)
8 ACAP(2)=-RRFX+(1.00/(RRFX-ACAP(1)))
TC1=ACAP(2)*RRFX+RX
TC2=ACAP(2)*RF+RX
FNA=(TC1*TA(3)-TA(1))/(TC1*WFN(2)-WFN(1))
FNB=(TC2*TA(3)-TA(1))/(TC2*WFN(2)-WFN(1))
FNAP=FNA
FNBP=FNB
T(1)=1.50
FROM HE-E TO T+E STATEMENT NUMBER 90, ELTRNX(I,J,K) HAS THE
FOLLOWING MEANING
ELTRMX(1,J,K)-REAL PART OF THE FIRST COMPLEX AMPLITUDE.
ELTRMX(2,J,K)-IMAGINARY PART OF THE FIRST COMPLEX AMPLITUDE.

```

```

C   ELTRMX(3,J,K)-REAL PART OF THE SECOND COMPLEX AMPLITUDE
CC   ELTRMX(4,J,K)-IMAGINARY PART OF THE SECOND COMPLEX AMPLITUDE.
K=1 FOR THETD(J) AND K=2 FOR 180.0-THETD(J)
DEFINITION OF THE COMPLEX AMPLITUDE-VAN DE HULST,P.125.
TB(1)=T(1)*TB(1)
TB(2)=T(1)*TB(2)
TC(1)=T(1)*TC(1)
TC(2)=T(1)*TC(2)
DO 9 J=1,JX
ELTRMX(1,J,1)=TB(1)*PI(2,J)+TC(1)*TAU(2,J)
ELTRMX(2,J,1)=TB(2)*PI(2,J)+TC(2)*TAU(2,J)
ELTRMX(3,J,1)=TC(1)*PI(2,J)+TB(1)*TAU(2,J)
ELTRMX(4,J,1)=TC(2)*PI(2,J)+TB(2)*TAU(2,J)
ELTRMX(1,J,2)=TB(1)*PI(2,J)-TC(1)*TAU(2,J)
ELTRMX(2,J,2)=TB(2)*PI(2,J)-TC(2)*TAU(2,J)
ELTRMX(3,J,2)=TC(1)*PI(2,J)-TB(1)*TAU(2,J)
ELTRMX(4,J,2)=TC(2)*PI(2,J)-TB(2)*TAU(2,J)
9  CONTINUE
QEXT=2.00*(TB(1)+TC(1))
QSCAT=(TB(1)**2+TB(2)**2+TC(1)**2+TC(2)**2)/0.75
CTBRCGS=0.00
N=2
10 T(1)=2*N-1
T(2)=N-1
T(3)=2*N+1
DO 11 J=1,JX
PI(3,J)=(T(1)*PI(2,J)*CSTHT(J)-N*PI(1,J))/T(2)
TAU(3,J)=CSTHT(J)*(PI(3,J)-PI(1,J))-T(1)*SI2HT(J)*PI(2,J)+TAU(1,J)
11 CONTINUE
WM1=WFN(1)
WFN(1)=WFN(2)
WFN(2)=T(1)*RX*WFN(1)-WM1
ACAP(1)=ACAP(2)
ACAP(2)=-N*RRFX+(1.00/(N*RRFX-ACAP(1)))
TC1=ACAP(2)*RRFX+N*RX
TC2=ACAP(2)*RF+N*RX
FNA=(TC1*TA(3)-TA(1))/(TC1*WFN(2)-WFN(1))
FNB=(TC2*TA(3)-TA(1))/(TC2*WFN(2)-WFN(1))
T(5)=N
T(4)=T(1)/(T(5)*T(2))
T(2)=(T(2)*(T(5)+1.00))/T(5)
CTBRCGS=CTBRCGS+T(2)*(TD(1)*TB(1)+TD(2)*TB(2)+TE(1)*TC(1)+TE(2)*TC(2)
1)+T(4)*(TO(1)*TE(1)+TO(2)*TE(2))
QEXT=QEXT+T(3)*(TB(1)+TC(1))
T(4)=TB(1)**2+TB(2)**2+TC(1)**2+TC(2)**2
QSCAT=QSCAT+T(3)*T(4)
T(2)=N*(N+1)
T(1)=T(3)/T(2)
K=(N/2)*2
DO 13 J=1,JX
ELTRMX(1,J,1)=ELTRMX(1,J,1)+T(1)*(TB(1)*PI(3,J)+TC(1)*TAU(3,J))
ELTPMX(2,J,1)=ELTRMX(2,J,1)+T(1)*(TB(2)*PI(3,J)+TC(2)*TAU(3,J))
ELTPMX(3,J,1)=ELTRMX(3,J,1)+T(1)*(TC(1)*PI(3,J)+TB(1)*TAU(3,J))
ELTPMX(4,J,1)=ELTRMX(4,J,1)+T(1)*(TC(2)*PI(3,J)+TB(2)*TAU(3,J))
IF (K.EQ.N) GO TO 12
ELTRMX(1,J,2)=ELTRMX(1,J,2)+T(1)*(TB(1)*PI(3,J)-TC(1)*TAU(3,J))

```

```

ELTRMX(2,J,2)=ELTRMX(2,J,2)+T(1)*(TB(2)*PI(3,J)-TC(2)*TAU(3,J))
ELTRMX(3,J,2)=ELTRMX(3,J,2)+T(1)*(TC(1)*PI(3,J)-TB(1)*TAU(3,J))
ELTPMX(4,J,2)=ELTRMX(4,J,2)+T(1)*(TC(2)*PI(3,J)-TB(2)*TAU(3,J))
GO TO 13
12 ELTRMX(1,J,2)=ELTRMX(1,J,2)+T(1)*(-TB(1)*PI(3,J)+TC(1)*TAU(3,J))
ELTRMX(2,J,2)=ELTRMX(2,J,2)+T(1)*(-TB(2)*PI(3,J)+TC(2)*TAU(3,J))
ELTRMX(3,J,2)=ELTRMX(3,J,2)+T(1)*(-TC(1)*PI(3,J)+TB(1)*TAU(3,J))
ELTRMX(4,J,2)=ELTRMX(4,J,2)+T(1)*(-TC(2)*PI(3,J)+TB(2)*TAU(3,J))
13 CONTINUE
IF (T(4).LT.1.00E-14) GO TO 15
N=N+1
DO 14 J=1,JX
PI(1,J)=PI(2,J)
PI(2,J)=PI(3,J)
TAU(1,J)=TAU(2,J)
PI(2,J)=PI(3,J)
TAU(1,J)=TAU(2,J)
TAU(2,J)=TAU(3,J)
14 CCNTINUE
FNAF=FNA
FNBF=FNBB
GO TO 10
15 DO 17 J=1,JX
DO 17 K=1,2
DO 16 I=1,4
T(I)=ELTRMX(I,J,K)
16 CCNTINUE
ELTRMX(2,J,K)=T(1)**2+T(2)**2
ELTRMX(1,J,K)=T(3)**2+T(4)**2
ELTRMX(3,J,K)=T(1)*T(3)+T(2)*T(4)
ELTRMX(4,J,K)=T(2)*T(3)-T(4)*T(1)
17 CCNTINUE
T(1)=2.00*RX**2
QEXT=QEXT*T(1)
QSCAT=QSCAT*T(1)
CTBROS=2.00*CTBROS*T(1)
THE DETAILS ABOUT THIS SUBROUTINE CAN BE FOUND IN THE FOLLOWING
REPCRT- SUBROUTINES FOR COMPUTING THE PARAMETERS OF THE
ELECTROMAGNETIC RADIATION SCATTERED BY A SPHERE J.V. DAVE,
IBM SCIENTIFIC CENTER, PALO ALTO, CALIFORNIA.
REPORT NO. 320 - 3237 . MAY 1968.
RETURN
18 FORMAT (T10,*THE VALUE OF THE SCATTERING ANGLE IS GREATER THAN
19 90.0 DEGREES. IT IS *,F15.4)
FORMAT (//T10,*PLEASE READ COMMENTS.*//)
20 FORMAT (//T10,*THE VALUE OF THE ARGUMENT JX IS GREATER THAN 100*)
21 FORMAT (//T10,*THE VALUE OF RFI.X IS GREATER THAN 80.0. IT IS *,F15.
14//)
END

```